Cretaceous Research 123 (2021) 104778

Contents lists available at ScienceDirect

Cretaceous Research

journal homepage: www.elsevier.com/locate/CretRes

# Macroids from mixed siliciclastic-carbonate high-frequency sequences of the Agrio Formation (Lower Cretaceous), Neuquén Basin: Palaeoecological and palaeoenvironmental constraints

Martina Caratelli [a, b, *], Fernando M. Archuby [a, c], Franz Fürsich [d], Johannes Pignatti [e]

[a] CONICET, Consejo Nacional de Investigaciones Científicas y Técnicas, Argentina
[b] IIPG- Instituto de Investigación en Paleobiología y Geología (Universidad Nacional de Río Negro – CONICET), Avenida Roca 1242, 8332, General Roca, Río Negro, Argentina
[c] Centro de Estudios Integrales de La Dinámica Exógena (CEIDE), Universidad Nacional de La Plata, Diagonal 113 Nro 469, 1900, La Plata, Buenos Aires, Argentina
[d] Fachgruppe Paläoumwelt, GeoZentrum Nordbayern der Universität Erlangen-Nürnberg, Loewenichstrasse 28, 91054, Erlangen, Germany
[e] Dipartimento di Scienze della Terra, Università di Roma "La Sapienza", Piazzale Aldo Moro 5, 00185, Roma, Italy

ARTICLE INFO

*Article history:*
Received 10 November 2020
Received in revised form
8 February 2021
Accepted in revised form 8 February 2021
Available online 17 February 2021

*Keywords:*
Lower Cretaceous
Agrio Formation
Benthic foraminifers
Sequence stratigraphy
Framboidal pyrite

ABSTRACT

Macroids, cm-sized biogenically coated grains made of associations of metazoans or protozoans, accumulate in some high-frequency sedimentary sequences of the upper Hauterivian to lower Barremian Agua de la Mula Member of the Agrio Formation in the Neuquén Basin (northern Patagonia, Argentina). The macroids studied are sub-spheroidal and sub-discoidal in shape, 2–3 cm in diameter and 1–2 cm in height. Each macroid is characterised by a rough, weakly bored surface, encrusted by oysters, serpulids, and small, dome-shaped bryozoan colonies. The growth arrangement consists of locally concentric, agglutinated encrusting foraminifers growing above and around skeletal nuclei. The accumulations of macroids on top of some starvation hemi-sequences during the latest Hauterivian 3rd-order transgressive systems tract help in understanding the palaeoenvironmental conditions at the onset of high-frequency regressions, characterised by low but persistent sedimentation rates and a generally low-energy environment. Mineralisation of sand-sized glauconite and apatite grains suggests ephemeral periods of reduced sedimentation or non-deposition. Pyrite framboid size-distribution indicates the upper dysoxic zone with oxygen restrictions. The re-establishment of terrigenous sediment input following transgression promoted eutrophication of the water column. Under such palaeoenvironmental conditions, benthic life was represented mainly by species able to thrive with eutrophicated, oxygen-poor waters at the sediment-water interface. This setting excludes activity of borers during the formation of macroids. Macroids result pivotal in understanding palaeoecology of inherent benthic communities and in refining the interpretation of palaeoenvironmental parameters in mixed siliciclastic-carbonate ramp systems.



## 1. Introduction

Coated grains, traditionally subdivided in biogenic and chemical precipitates, consist of cm-sized carbonate and non-carbonate material. They occur in a wide variety of environments ranging from shallow to deep sea. Among the biogenically coated grains, oncoids, rhodoliths, and macroids represent the most common grain types. They are composed of an organic or inorganic nucleus coated by diverse biogenic envelopes arranged in a great variety of growth forms (e.g., Bosellini and Ginsburg, 1971; Bosence, 1983; Čatalov, 1983; Flügel, 2004). Like chemical coated grains, biogenic ones have been recognised as useful palaeoecological and palaeoenvironmental indicators (e.g., Bosence, 1983; Scoffin et al., 1985; Reid and Macintyre, 1988; Toomey et al., 1988). Classification of biogenically coated grains is mainly based on differentiating biotic constituents. Presently, red algae are considered to be main

* Corresponding author. CONICET, Consejo Nacional de Investigaciones Científicas y Técnicas, Argentina.
*E-mail addresses:* mcaratelli@unrn.edu.ar (M. Caratelli), farchuby@fcnym.unlp.edu.ar (F.M. Archuby), franz.fuersich@fau.de (F. Fürsich), johannes.pignatti@uniroma1.it (J. Pignatti).

https://doi.org/10.1016/j.cretres.2021.104778
0195-6671/

constituent of rhodoliths, while non-red algae, cyanobacteria, and bacteria represent the dominant component of oncoids (e.g., spongiostromate and porostromate oncoids; Peryt, 1983). When encrusting metazoans or protozoans (occasionally associated with coralline algae) are significant constituents of cm-sized (>10 mm) coated grains, these biogenic nodules are named macroids (Hottinger, 1983; Peryt, 1983; Flügel, 2004). Calcareous and/or agglutinated encrusting foraminifers are the dominant constituents of macroids, forming randomly arranged growth forms attached to hard surfaces such as bioclasts. These macroid pavements are commonly found both in modern environments and in the fossil record. Examples from Recent tropical marine depositional settings are macroids formed by encrusting foraminifers and coralline red algae, termed both 'foraminiferal algal nodules' and 'for-algaliths' (e.g., Reid and Macintyre, 1988; Prager and Ginsburg, 1989; Bassi et al., 2012). Foraminiferal macroids ('zoogenic oncoids'; Čatalov, 1983) formed by the hyaline genera *Acervulina*, *Gypsina* and the agglutinated genus *Haddonia* are common constituents of Cenozoic reef carbonates (e.g., Perrin, 1992; Bosellini and Papazzoni, 2003; Varrone and d'Atri, 2007). Large bioherms up to 1 m in height extending for several kilometres framed by the agglutinated foraminifer *Bdelloidina* occur in the Lower Cretaceous inner carbonate platform facies of the Urgonian of Haute-Savoie, France (e.g., Schulte et al., 1993; Wernli and Schulte, 1993). Cyanobacteria and algae associated with encrusting foraminifers have been described from the Upper Frasnian unit of Belgium (Denayer, 2018) and the lower Permian units of southern Kansas, northern Oklahoma, Texas, and southern New Mexico, variously named 'algal biscuits' and 'osagic grains' (e.g., Johnson, 1946; Toomey et al., 1988; Scholle et al., 2016). Major attention was also paid to the study of the role of encrusting foraminifers in the growth of deep-sea non-carbonate macroids (i.e., manganese nodules) and crusts, since the discovery of these firmgrounds (e.g., Wendt, 1969; Tucker, 1973; Greenslate, 1974; Dugolinsky et al., 1977; Mullineaux, 1988; Pattan, 1993). Several benthic foraminifers have been observed attached to manganese nodules and interpreted as active builders of such nodules. Commonly, dark 'pillar-like structures' or 'stromatolitic' columns are the accretionary growth structures built up by agglutinated encrusting foraminifers (e.g., Wendt, 1974; Hornung et al., 2007; Rodríguez-Martínez et al., 2011; Scholle et al., 2016).

Trophic resources, defined by Hallock (1987) as nutrients available to primary producers and organic carbon available to consumers, constituting the trophic resource continuum (TRC), have been recognized as highly relevant in shaping the configuration of communities and their development through time. A low trophic resource level, known as oligotrophy, is associated with highly complex and diverse communities, while at the other end of the continuum, eutrophic waters promote the development of low-diverse biocoenoses dominated by opportunistic species, with low preservation potential. Besides, high levels of nutrients and organic matter might generate a reduction in available oxygen that introduces further stress to the ecosystem (Hallock, 1987, 1988; Lukasik et al., 2000).

Macroids were mentioned by Archuby (2009) and Archuby and Fürsich (2010) from two different stratigraphic sections (i.e., Agua de la Mula and Bajada del Agrio) of the upper Hauterivian to lower Barremian Agua de la Mula Member of the Agrio Formation (Neuquén Basin, northern Patagonia, Argentina). The authors reported 'nodular foraminiferal buildups' forming knobby pavements and dome-like structures in terrigenous sediment-starved deposits. Although agglutinated encrusting foraminifers are common in terrigenous starved beds, the presence and eventual accumulation of macroids is exceptional occurring on top of some starvation hemi-sequences (*sensu* Archuby and Fürsich, 2010) in relatively deep settings tending to eutrophication. Records of encrusting foraminifers from the Agua de la Mula Member are limited to the calcareous taxon *Webbinella* sp. (Ballent et al., 2006) and to an agglutinated specimen referred to *Tolypammina vagans* Brady encrusting a nautiloid shell (Luci and Cichowolski, 2014).

The Agua de la Mula Member in the study area constitutes the infill of a siliciclastic and mixed siliciclastic-carbonate homoclinal ramp system in a proximal position within the Neuquén Basin (Spalletti et al., 2001; Archuby et al., 2011). Oligotrophic carbonates (i.e., coral reefs) are restricted to the top of the member. Conversely, siliciclastic-dominated intervals fed by a regular supply of terrigenous sediments and deposited under more eutrophic conditions are widespread in the sedimentary succession. The palaeogeographic context suggests a warm-temperate climate, during which sedimentary facies were punctuated by high-frequency (6th-order) sequences dominated by thin transgressive systems tracts and thick regressive (progradational) highstand systems tracts (Sagasti, 2005; Archuby and Fürsich, 2010; Archuby et al., 2011; Guler et al., 2013). New surveys of the Agua de la Mula and Bajada del Agrio localities allowed us to obtain additional data for the characterisation of these macroids with regard to both, the encrusting fauna and associated (bio)mineralisations (i.e., spherical clusters of framboidal pyrite and glauconite). Here, we take a closer look at the material previously reported by Archuby (2009) and Archuby and Fürsich (2010) in order to (1) describe the distinct encrusting assemblages and their growth forms, (2) characterise the (bio)mineralisations, (3) evaluate the occurrence of macroids along the upper Hauterivian sedimentary sequences, and (4) provide new evidence to improve the interpretation of the palaeoecological and palaeoenvironmental significance of the encrusting community forming macroids in the Agua de la Mula Member.

## 2. Geological setting

The Neuquén Basin is a triangular-shaped basin located on the eastern side of the Andes (west-central Argentina), between latitudes 32° and 40° S (Fig. 1). The basin is filled with an up to 7000-m-thick Upper Triassic–lower Cenozoic sedimentary succession recording a wide variety of depositional settings (Legarreta and Uliana, 1991; Howell et al., 2005; Schwarz et al., 2016). The sedimentary fill of the Neuquén Basin accumulated during different tectonic phases, including syn-rift, post-rift and foreland stages (Legarreta and Uliana, 1991; Vergani et al., 1995; Howell et al., 2005). The Agrio Formation (early/late Valanginian-early Barremian) represents the last unit of the Mendoza Group, which records the post-rift infill during the back-arc stage of the Neuquén Basin (Vergani et al., 1995; Howell et al., 2005). The unit is widespread in the Neuquén Basin both in outcrop and subsurface, from the northern Mendoza Province to the southern Huincul Ridge (Leanza et al., 2001; Spalletti et al., 2001, 2011). It conformably overlies the marine and continental deposits of the Mulichinco Formation (Valanginian) and is covered discordantly by sandstones, evaporites and limestones of the Huitrín Formation (Barremian). It has traditionally been divided into three members (Weaver, 1931; Leanza et al., 2001): the (lower) Pilmatué, (middle) Avilé, and (upper) Agua de la Mula. The lower and upper members of the unit consist of thick, richly fossiliferous, rhythmic successions made of marine mixed siliciclastic and carbonate deposits (i.e., mudrocks, marlstones, limestones, sandstones) separated by the Avilé continental sandstones (Leanza et al., 2001; Archuby and Fürsich, 2010; Archuby et al., 2011; Spalletti et al., 2011).

The Agua de la Mula Member (late Hauterivian–early Barremian), which contains the deposits analysed, is an up to 1000-m-thick package of distal (low sedimentation rate dominated) mixed siliciclastic-carbonate to proximal (high sedimentation rate dominated) ramp deposits (Spalletti et al., 2001; Archuby and

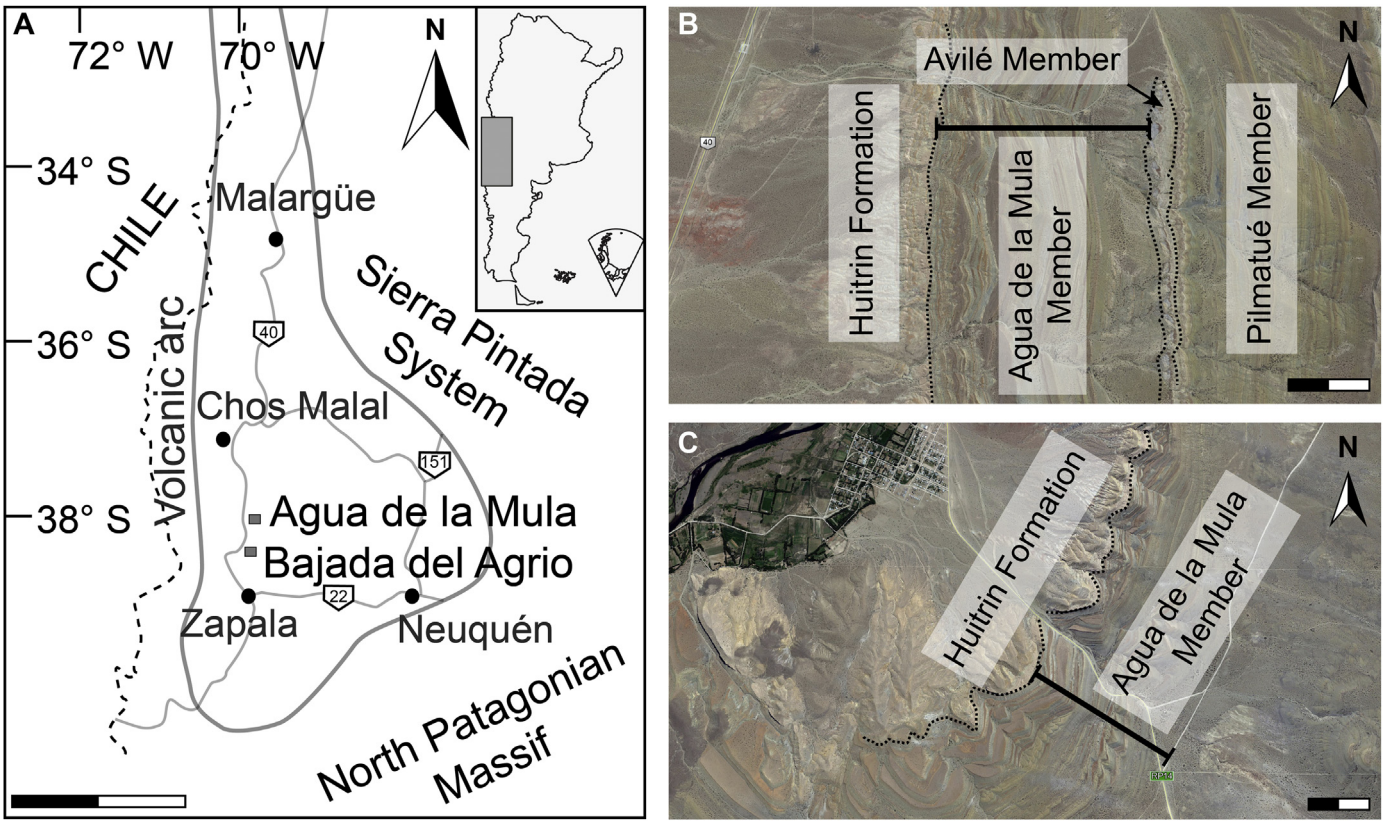


**Fig. 1.** A) Geographic position of the Neuquén Basin and location of the measured stratigraphic sections, Agua de la Mula and Bajada del Agrio (modified from Archuby et al., 2009). Grey solid line: Neuquén Basin boundary; thinner grey lines: National Routes; dotted line: political boundary between Chile and Argentina. Scale bar = 200 km. B, C) Google Earth satellite images showing the outcrops of the Agua de la Mula Member at Agua de la Mula (B) and Bajada del Agrio (C) sections. Dotted lines: lithostratigraphic boundaries; black solid segments: transect of sampled sections. Scale bars = 500 m.

Fürsich, 2010; Archuby et al., 2011). The unit constitutes, together with the lower and middle members of the Agrio Formation, a 2nd-order sedimentary sequence (Upper Mendoza Mesosequence; Legarreta and Gulisano, 1989; Legarreta and Uliana, 1991; Spalletti et al., 2001). The marine deposits of the upper member are embedded between two continental lithostratigraphic units recording important regressive packages, the Avilé Member below and the Huitrín Formation above. The deposition of the Agua de la Mula Member begins with the re-establishment of marine conditions following the relative sea-level drop documented by the abrupt deposition of fluvial sandstones of the Avilé Member above the deep marine shales of the Pilmatué Member (Veiga et al., 2002). High-frequency cyclicity is an outstanding feature of the Agua de la Mula Member (Legarreta and Gulisano, 1989; Legarreta and Uliana, 1991; Spalletti et al., 2001; Archuby and Fürsich, 2010; Archuby et al., 2011). In the northern to southern Neuquén Basin, various examples of high-frequency cyclicity of the Agua de la Mula Member clearly stand out in the stratigraphic sections, from the southern Mendoza province (Sagasti, 2000) to the northern and central Neuquén province (Loma La Torre and Bajada del Agrio sections; Spalletti et al., 2001; Archuby and Fürsich, 2010; Archuby et al., 2011; Comerio et al., 2019; Kietzmann and Paulin, 2019).

### 2.1. Stratigraphic sections

Two stratigraphic sections of the Agua de la Mula Member of the Agrio Formation, i.e. Bajada del Agrio and Agua de la Mula (hereafter BAL and AM respectively), were measured (Fig. 2). Both sections conformably overlie the medium-to coarse-grained continental sandstones of the Avilé Member (Fig. 3A, B). The top of the unit is well marked by fluvial coarse-grained sandstones and gypsum layers of the Huitrín Formation at the Bajada del Agrio locality and is poorly exposed at the Agua de la Mula locality (Fig. 3C, D). Both sections consist of thin-bedded dark shales and argillaceous marlstones intercalated between bioclastic carbonates (grainstone/packstone and locally floatstone to rudstone) and subordinated sandstones (Archuby and Fürsich, 2010; Spalletti et al., 2011 and references therein).

#### 2.1.1. Bajada del Agrio section

The section is situated on the right side of the Agrio river, approximately 10 km southwest of the locality Bajada del Agrio, along the Provincial route 14 (Fig. 1). The base of the section consists of laminated dark shales and marly shales resting on ripple-laminated fine-to medium-grained sandstones and siltstones with desiccation cracks of the Avilé Member. Dark marlstones and marly shales, with a dispersed benthic macrofauna of gastropods, bivalves, and echinids and interbedded shell beds (25–90 cm in thickness), and fine-grained bioturbated sandstones (3–5 cm in thickness) dominate the first 200 m of the section (*Spitidiscus riccardii* and lower part of *Crioceratites schlagintweiti* Zone; Aguirre-Urreta, 1995; Aguirre-Urreta and Rawson, 1997). Fine-grained ripple-laminated sandstones occur in the uppermost few metres. They are followed by high-frequency sequences consisting of rhythmic alternations of dark mudrocks and siltstones with fine-to medium-grained condensed sandstones (20–40 cm in thickness) (upper part of the *C. schlagintweiti* and *C. diamantensis* Zone; Aguirre-Urreta

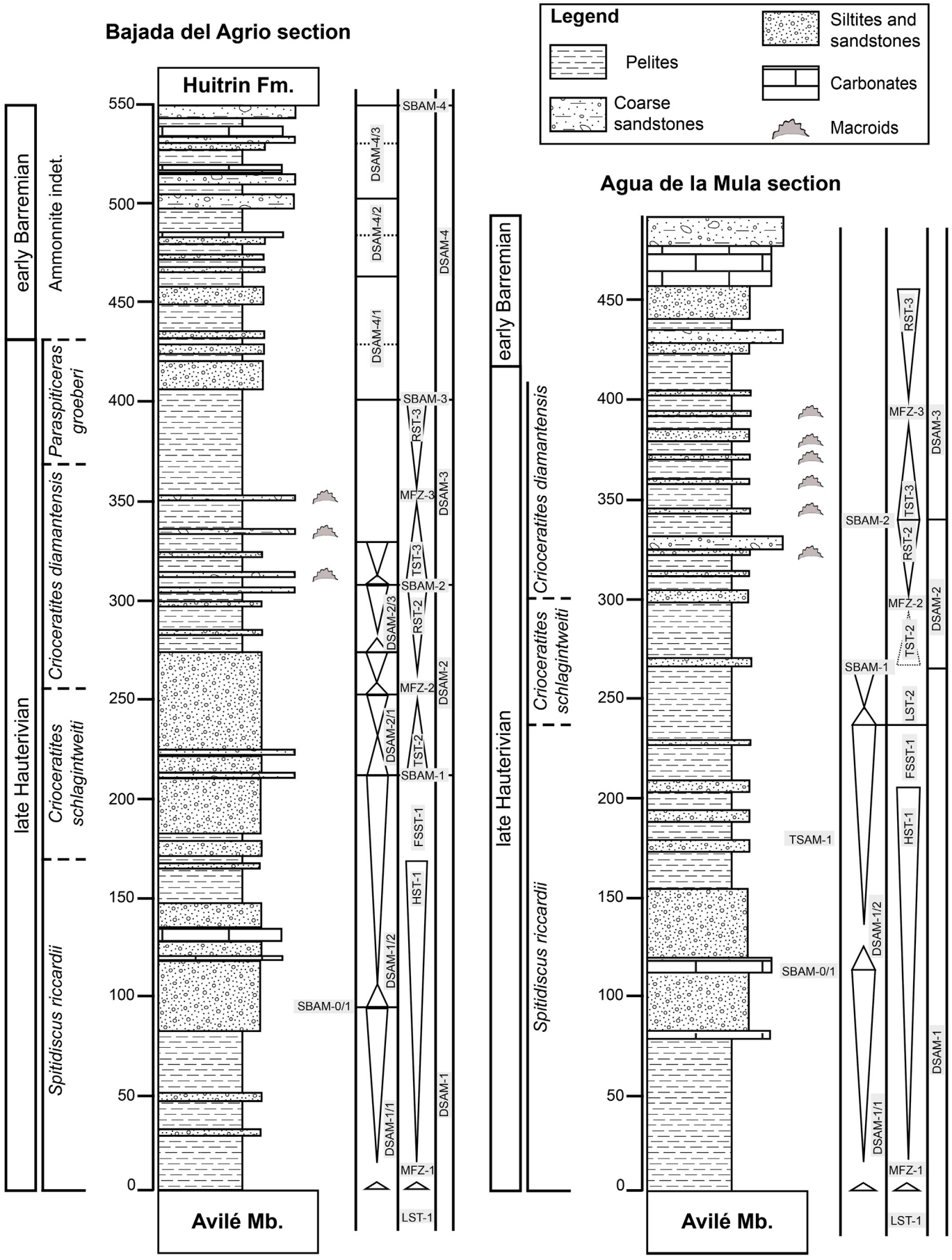
Legend
Siltites and sandstones
Pelites
Carbonates
Coarse sandstones
Macroids
Bajada del Agrio section
Huitrin Fm.
Avilé Mb.
early Barremian
late Hauterivian
Ammonite indet.
Paraspiticeras groeberi
Crioceratites diamantensis
Crioceratites schlagintweiti
Spitidiscus riccardii
550
500
450
400
350
300
250
200
150
100
50
0
SBAM-4
SBAM-3
SBAM-2
SBAM-1
SBAM-0/1
DSAM-4/3
DSAM-4/2
DSAM-4/1
DSAM-4
DSAM-3
DSAM-2/3
DSAM-2/1
DSAM-2
DSAM-1/2
DSAM-1/1
DSAM-1
RST-3
MFZ-3
TST-3
RST-2
MFZ-2
TST-2
FSST-1
HST-1
MFZ-1
LST-1
Agua de la Mula section
Crioceratites diamantensis
Crioceratites schlagintweiti
Spitidiscus riccardii
450
400
350
300
250
200
150
100
50
0
TSAM-1
SBAM-2
SBAM-1
SBAM-0/1
RST-3
MFZ-3
TST-3
RST-2
MFZ-2
TST-2
LST-2
FSST-1
HST-1
MFZ-1
LST-1
DSAM-3
DSAM-2
DSAM-1/2
DSAM-1/1
DSAM-1
Avilé Mb.

**Fig. 2.** Simplified stratigraphic sections of the Agua de la Mula Member (see Archuby and Fürsich, 2010 for further details) with locations of the macroid deposits/pavements. Ammonite biozones and sequence stratigraphy from Archuby et al. (2009). DSAM: Depositional sequence of the Agua de la Mula Member; LST: Lowstand systems tract; MFZ: Maximum flooding zone; HST: Highstand systems tract; FSST: Falling stage systems tract; SBAM: Sequence boundary within the Agua de la Mula Member; TST: Transgressive systems tract; RST: Regressive systems tract; TS: Transgressive surface.

and Rawson, 1997). Heterolithic and hummocky cross-stratified sediments and bioturbated fine-grained sandstones are common features of the upper part of the *C. diamantensis* Zone. Thin knobby pavements made of macroids occur within a 40-m-thick interval (from ca. 310–350 m; Fig. 2) and rest on the top of some condensed beds, the latter consisting of coarse-grained mixed rocks (e.g., sandy allochemic limestones, bioclastic sandstones; *C. diamantensis* Zone). Above, a marked increase in carbonate content is recorded by limestones, marly limestones, and calcareous marlstones interbedded between poorly bioclastic mudrocks and subordinate fine- to medium-grained sandstones with ripple lamination (*Parastpiticeras groeberi* Zone; Aguirre-Urreta et al., 2005). Thick oolitic beds (2–5 m in thickness) with grainstone/packstone textures are important constituents of this last part of the section). They are composed of poorly sorted ferruginous ooids and shell fragments scattered in a fine-grained siliciclastic matrix. Glauconite grains also occur. Small and scattered coral patch reefs rest at the top of the condensed sandstones. Barren medium-grained sandstones with ripple lamination occur just below the sandstone and gypsum layers of the Huitrín Formation. The boundary is a low-angle unconformity.

*2.1.2. Agua de la Mula section*

The AM section is located ca 90 km south of the locality Chos Malal, Neuquén Province, approximately 5 km east of National Route 40 (Fig. 1). Dark sandy calcareous shales and marlstones, rich in gastropods and articulated bivalves, with intercalated thin, fine-to medium-grained sandstones (*Spitidiscus riccardii* Zone; Aguirre-Urreta, 1995; Aguirre-Urreta and Rawson, 1997) overlie medium-to coarse-grained sandstones of the Avilé Member. Thin, loosely packed shell beds also occur. As in the BAL section, they are followed by high-frequency sequences consisting of rhythmic alternations of dark bioturbated mudrocks/siltstones and thick fine- to medium-grained condensed sandstones (30–80 cm in thickness) (*C. schlagintweiti* and lower part of the *C. diamantensis* Zone; Aguirre-Urreta and Rawson, 1997). Ripple- and hummocky cross-stratified fine-to medium-grained sandstones dominate the upper portion of this interval. Characteristically, the macrofauna of the sediment-starved basal beds of each high-frequency sequence is mainly composed of gastropods and bivalves and contains ammonites, their upper surfaces encrusted by oysters and serpulids. Glauconite grains are also present. Macroids generally occur at the top of thick and complex starvation hemi-sequences within a 55-m-thick interval (from 330 up to 385 m; Fig. 2) (*C. diamantensis* Zone). In some cases, densely packed accumulations of macroids form domal structures ranging from a few decimetres to 1 m. Poorly fossiliferous fine-grained carbonate sandstones and marlstones, and interbedded bioturbated calcareous mudrocks and subordinate siltstones characterise the upper part of the *C. diamantensis* Zone. Oolitic beds (20–50 cm in thickness) with grainstone/packstone texture and associated micritic bioclastic floatstones and rudstones record an increased carbonate content up-section. Ferruginous ooids and glauconite grains are common constituents of the rocks. Coral patch reefs occur at the top of the oolitic beds. Fine-grained mudrocks are intercalated between fine- to medium-grained sandstones with ripple and hummocky cross-lamination up to ca. 430 m of the section. The last part of the section is poorly exposed and barren. Fine-grained sandstones probably belonging to the overlying Huitrín Formation were observed.

## 3. Material and methods

Macroids analysed in this study were collected at the localities Bajada del Agrio and Agua de la Mula, in the transgressive systems tract of the 3rd-order sedimentary sequence DSAM-3 (Archuby et al., 2011). Samples were observed under the binocular microscope; thin-sections were examined and described with the optical microscope Nikon Eclipse E200 and were also studied under the Philips XL20 Scanning Electron Microscope (SEM). Besides, energy-dispersive X-ray (EDX) spectra and element mapping were performed in order to characterise the morphology and test mineralogy of encrusting agglutinated foraminifers and pyrite framboids. The semi-quantitative chemical analysis was performed with a voltage of 20 kV. Measurements of framboid diameters and sizes were taken from selected SEM pictures. Repository: Museo Provincial de Ciencias Naturales "Dr. Prof. Juan A. Olsacher", Zapala, Neuquén Province, Argentina. Paleomicroinvertebrates collection. Institutional abbreviation: MOZ-Pm.

## 4. Description of macroids

Macroids consist of cm-sized nodules, sub-spheroidal/subdiscoidal in shape, formed by an assemblage of benthic macrofaunal remains and an encrusting community of microorganisms, mainly agglutinated foraminifers and associated bryozoans and serpulids (Fig. 4). Typical continuous laminations made of algal encrusters are missing. Each macroid, being 2–3 cm in diameter and 1–2 cm in height, was for the major part built by agglutinated encrusting foraminifers that grew attached to nuclei composed of skeletal remains, mostly oyster and other, undetermined, bivalve bioclasts. Macroids form pavements occurring both separated from each other in a fine-grained siliciclastic matrix and in large clusters.

*4.1. Macroscopic and thin-section analysis*

The external surface of macroids is generally rough and weakly bored, and encrusted by oysters and bryozoans. The encrusting bryozoans are fairly well-preserved, most of them showing affinities with the Lower Cretaceous cyclostome fauna reported from the Agrio Formation (Taylor et al., 2009). Colonies consist of flat and warty small masses less than 3 mm thick, cemented to the skeletal substrate composed of oysters and other bivalve bioclasts (Fig. 5A). Tubular zooids with ovoidal apertures are visible. The bryozoan colonies are up to 5 mm in diameter and are separated from each other by a few mm. Also, solitary serpulids consisting of long, convoluted tubes with meander turns and smooth surfaces co-occur with bryozoans on the macroid surfaces (Fig. 5B).

Internally, agglutinated foraminifers encrust skeletal nuclei, growing irregularly and producing complex structures (Fig. 6A, B). In some cases, bioclastic nuclei are coated with pyrite framboids seen on foraminiferal attachment surfaces (Fig. 6C) and, in contrast to the external macroid surface, nuclei have not been affected by bioerosion. As is well known, growth and development of the encrusting foraminiferal tests reflect the morphology of their substrate, both inorganic (i.e., hardgrounds, Mn-nodules, debris material; e.g., Mullineaux, 1988; Gischler and Ginsburg, 1996; Resig and Glenn, 1997) and organic (i.e., hardparts of invertebrates; e.g., Kidwell and Jablonski, 1983; Jones and Hunter, 1995; Richardson-White and Walker, 2011), producing irregularly and variably arranged chambers. In some of our examples, the shape of the

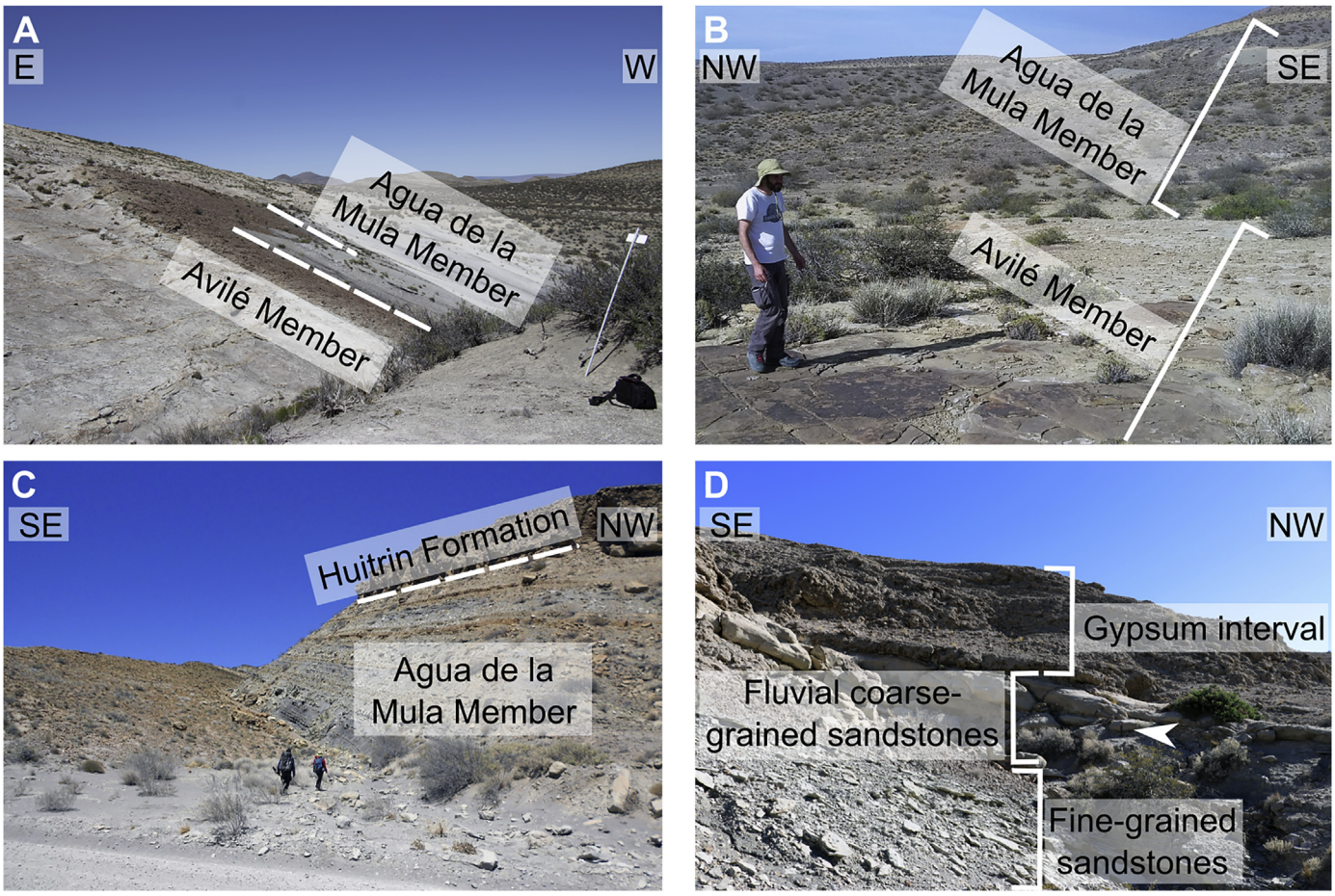


**Fig. 3.** A, B) Basal contact between the Agua de la Mula Member and continental sandstones of the Avilé Member at the AM (A) and BAL (B) sections. C) Upper contact between the Agua de la Mula Member and the Huitrín Formation at the BAL section. D) Detail of the uppermost part of the BAL section showing coarse-grained fluvial sandstones (Lower Troncoso Member) and gypsum (Upper Troncoso Member) layers of the Huitrín Formation unconformably overlying fine-grained sandstones of the Agua de la Mula Member.

foraminiferal attachment surfaces reflects the concavo-convex pattern of the bioclast they encrust (Fig. 6D). The initial convex-upward growth of the encrusting foraminifers took place on any point of the available bioclast surface, in a similar way to that described by Wendt (1974), Toomey et al. (1988), and Scholle et al. (2016). Two main growth forms were observed: (1) a densely curved morphology consisting of superimposed agglutinated encrusting foraminiferal tests (Fig. 6E), and (2) a gentle wavy morphology of foraminiferal encrustations with a fashion similar to small-scale stromatolitic structures (Fig. 6F) (e.g., Wendt, 1969; Tucker, 1973; Rodríguez-Martínez et al., 2011). Size of the tests and shape of the chambers are very irregular in both cases. The proximity and overlap between different foraminiferal tests produce strongly variable outlines of macroids in thin-sections. Test arrangement as tangled masses makes it difficult to trace and identify the growth of individuals from randomly oriented thin-sections. Some specimens of encrusting foraminifers tentatively have been compared with the genera *Haddonia* Chapman, 1898 (Family Haddoniidae), *Alpinophragmium* Flügel, 1967, *Bdelloidina* Carter, 1877 and *Coscinophragma* Thalmann, 1951 (Family Coscinophragmatidae). For the time being, these studied specimens are considered to differ from the above-mentioned genera and are kept in open nomenclature. An in-depth characterisation of proloculus and apertures is still missing but required to resolve the taxonomic and systematic position of the specimens. Elongate depressions similar to slight pits locally separate foraminiferal growth stages around skeletal nuclei (Fig. 6G). These columnar areas are filled with the same fine-grained siliciclastic matrix occurring between macroids and contains fine-bioclastic debris. Agglutinated tubular foraminifers with an imperforate arenaceous wall (*Tolypammina*?) are also associated. Encrusting foraminifers with calcareous test were not observed, while infaunal benthic foraminifers are rare in the matrix, represented by rare polymorphinids.

### 4.2. SEM analysis

SEM semiquantitative analysis revealed that pyrite framboids occur scattered in the fine-grained siliciclastic matrix as well as filling the chambers of the encrusting foraminifera. In some cases, framboids were observed coating the bioclasts surrounded by foraminiferal encrustations. Framboids show a wide size distribution ranging from 2.5 to 25 μm in diameter (mean size 9.5 μm), but most of them range from 8 to 10 μm. EDX spectra show that the smallest fraction of framboids (<6 μm) preserves the original pyrite composition, while in the remaining ones degradation of sulphur concentration is a common feature (Fig. 7) leading to the formation of iron oxyhydroxide. This pseudomorphic transformation affected the original chemical composition of pyrite due to subsequent exhumation and exposure to oxygenated waters (e.g., Merinero et al., 2009, 2010), but preserved the original framboidal morphology and size distribution. Authigenic glauconite also

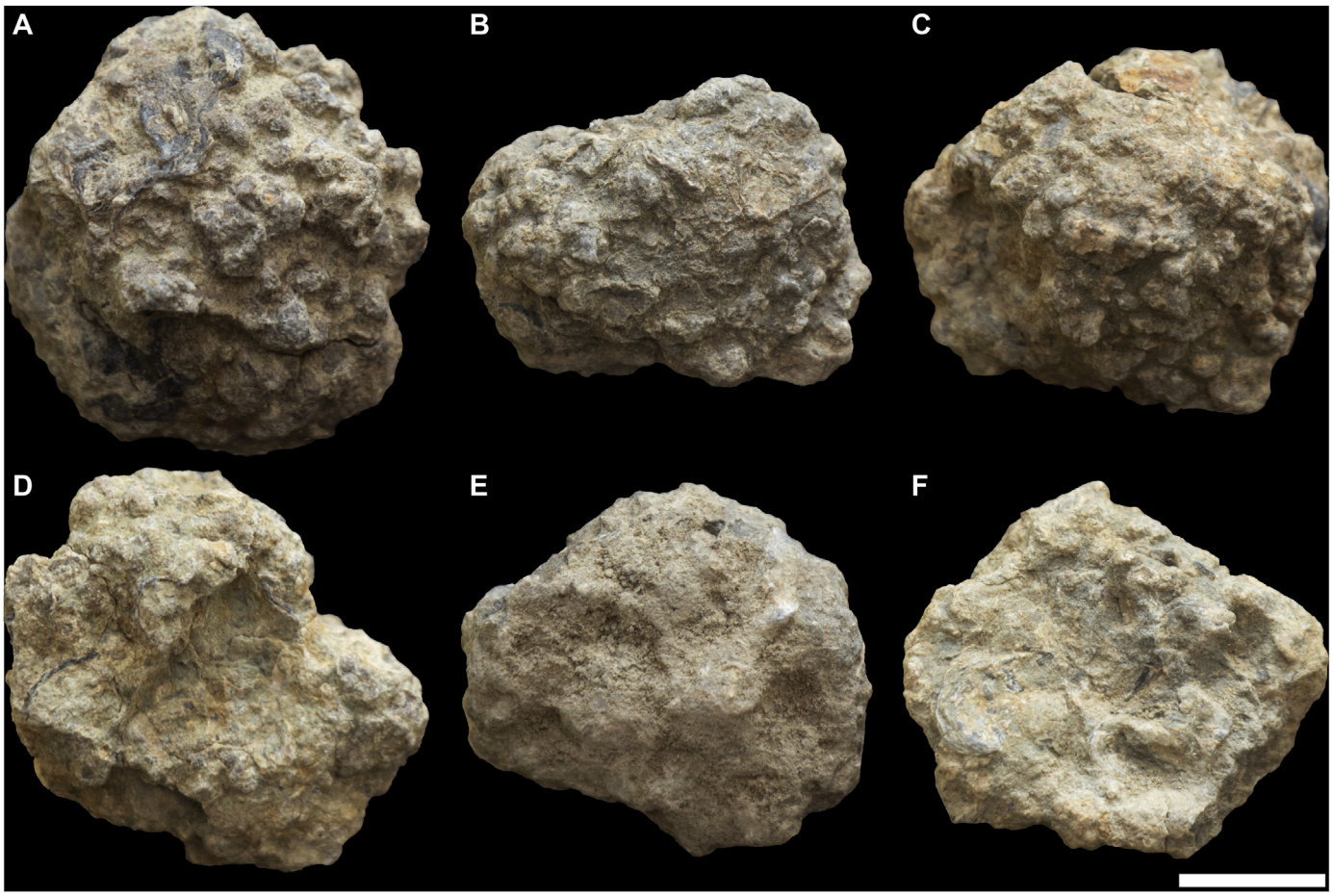


**Fig. 4.** Macroids from the AM section showing the characteristic sub-spheroidal and sub-discoidal shapes. A-C) Outer surface with the characteristic warty protuberances. D-F) Lower side with weakly flattened and depressed area in the centre. Encrusting oysters are visible on both sides of the macroids. Scale bar = 1 cm. Collection numbers: MOZ-Pm 001 (A); MOZ-Pm 002 (B); MOZ-Pm 003 (C); MOZ-Pm 004 (D); MOZ-Pm 005 (E); MOZ-Pm 006 (F).

occurs, scattered in the siliciclastic matrix as dark-green sand-sized grains.

Foraminiferal tests show clear peaks of Si, Al, Na, K, Ca, P and traces of Fe (Fig. 8). Wall test composition is dominated by Si, with subordinate Al, Na, and K, consistent with an agglutinated test (sand and silt grains). Wall test thickness is 0.05 to 0.020 mm. High content of Si suggests the presence of detrital quartz as dominant component of the tests, while Al, Na, and K suggest feldspar grains and clay particles as additional components. Ca and in minor proportion P are dominant within the foraminiferal chambers, suggesting calcite and apatite as common fill minerals. Traces of Fe are related to framboidal pyrite that locally replaced the infilling.

## 5. Discussion

Macroids of the upper Hauterivian marine beds of the Neuquén Basin stand out in being fully constructed by encrusting agglutinated foraminifers, developing a peculiar (half) nut-like shape. It is well known that such biogenic structures are valuable tools to refine the interpretation of environmental parameters that control sea floor conditions (e.g., Wendt, 1969, 1974; Tucker, 1973; Reid and Macintyre, 1988; Toomey et al., 1988; Rodríguez-Martínez et al., 2011). The macroids studied provide information on sedimentation rate, oxygen level, and water energy during deposition of 3rd-order transgressive systems tracts, allowing to integrate these parameters with previous sequence-stratigraphic reconstructions and to better characterise important shifts in the depositional dynamics.

### 5.1. Palaeoenvironmental interpretation

#### 5.1.1. Sedimentation rate and water energy

Internal growth fabric of the Agua de la Mula Member macroids resembles both 'algal-foram growth' and 'pillar-like structures', described by Toomey et al. (1988) and Wendt (1969), respectively although differing in some aspects. In our case study, the complex arrangement of agglutinated encrusting foraminifers reveals unbroken surfaces of the foraminiferal tests suggesting that no interruption of growth occurred. Unlike the 'pillar-like structures' found in the Carnian Hallstatt Limestones (Wendt, 1969, 1974), where the accretionary growth of organic microstructures is interrupted by deposition of ferromanganese crusts, our macroids show no evidence of such hard surfaces in spite of the similarities in the geochemical composition. Ferromanganese crusts and nodules are common in poorly oxygenated marine depositional settings, characterised by very low sedimentation rates and submarine erosion in sediment-starved environments (e.g., Jenkyns, 1970; Kennedy and Garrison, 1975; Fürsich et al., 1992; Wilson and Palmer, 1992; Fürsich and Pandey, 2003; Taylor and Wilson, 2003). As documented by Rodríguez-Martínez et al. (2011), settings with very low sedimentation rates offered suitable substrates for the growth of *Tolypammina* columns or pillar clusters, while under moderately reduced sedimentation rates, foraminiferal

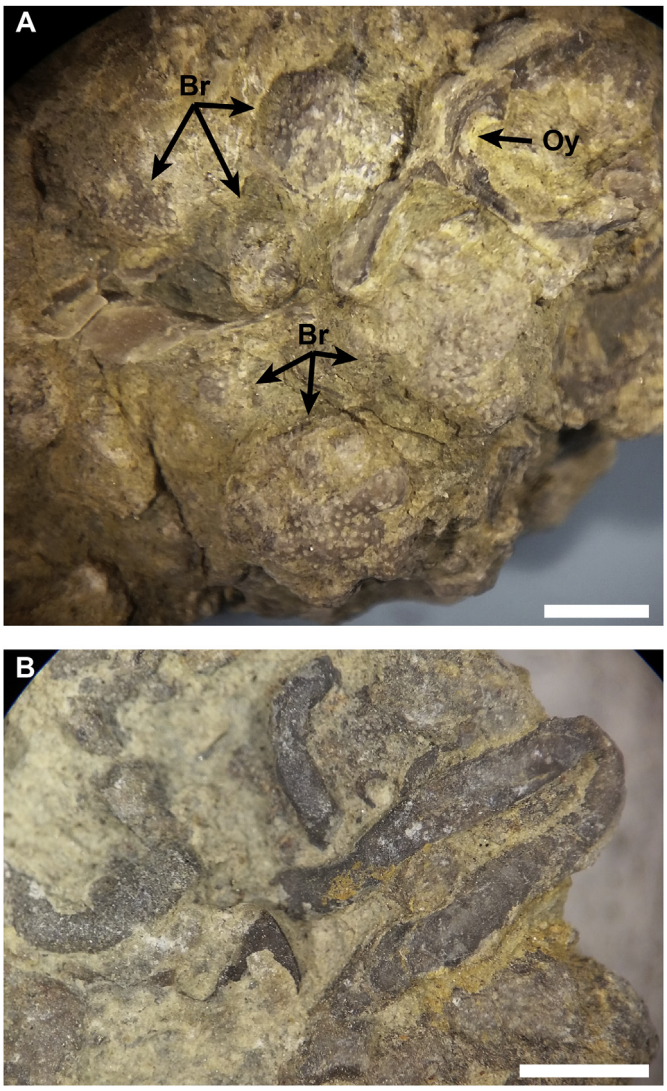


**Fig. 5.** A) Bryozoan colonies encrusting oyster bioclasts. Bryozoan tubular zooids with ovoid apertures are preserved. B) Convoluted tubes of serpulids growing across the macroid surface. Br: bryozoan colonies; Oy: oysters. Scale bars = 2 mm. Collection number: MOZ-Pm 007 (A-B).

colonies are less widespread, although *Tolypammina* individuals are present. Many authors have long discussed the role played by encrusting foraminifers in the formation of ferromanganese crusts and nodules (e.g., Greenslate, 1974; Wendt, 1974; Dugolinsky et al., 1977; Mullineaux, 1988). A possible active role of foraminifers in ferromanganese precipitation has been suggested for Recent and fossil manganese nodules, leading to the general view that foraminifers can secrete organically bound iron cement. Moreover, several cases of framboidal pyrite filling chambers or tests of microfossils have been reported from marine sedimentary rocks of different ages and related to diagenetic processes (e.g., Love and Murray, 1963, 1984; Love, 1971; Pollastro, 1981; Shroba, 1993). Examples of pyrite framboids disseminated throughout sedimentary facies and partially replacing shells or infilling foraminiferal chambers have been already reported from the Agua de la Mula Member (e.g., Sagasti, 2000; Archuby, 2009; Comerio et al., 2018, 2020). The occurrence of framboids is often closely associated with the availability of organic matter, both present in the surrounding sediment as well as forming the soft parts of the fossil "hosts" (e.g., foraminifers, ostracods, phytoplankton). Remains of organisms represent the prime nourishment for sulfate reducing bacteria, thus promoting iron sulfide deposition (Brett and Allison, 1998). Physico-chemical reactions during burial, or soon after, occurring on the organic matter present both in the siliciclastic matrix and in the interior of the foraminifera chambers are generally invoked for the formation of diagenetic pyrite framboids (Berner, 1984).

In our examples, the products of bacterial activity (i.e., pyrite framboids) were observed as (1) infilling of foraminiferal chambers and (2) in-between bioclasts and foraminiferal tests. In the first case, where foraminiferal chambers acted as receptacles for framboidal pyrite, bacterial activity likely occurred during early diagenesis. The possibility that foraminifers were alive at the time of bacteria activity cannot be totally dismissed, based on findings of iron concentrations in the foraminiferal protoplasm in laboratory cultures (e.g., Hedley, 1963; Leiter and Altenbach, 2010). In the second case, the remarkable arrangement of framboidal pyrite allows us to speculate on the role played by encrusting foraminifers during framboid formation, as well as on the possible relationship between foraminifers and bacteria. We observed cases, in which bivalve bioclasts encrusted by agglutinated foraminifers show framboids occurring at the start of foraminiferal test growth (Fig. 6C, E). Pyrite framboids appear encased between the external surfaces or localised points of encrusted bivalve fragments and foraminifers, making these mineral aggregates a clue for likely bacterial-foraminiferal interaction. Evidence supports the idea that organic molecules secreted by foraminifers may have encouraged the activity of sulfate reducing bacteria, thus promoting iron-sulfide production. In this view, organic substances (i.e., acid mucopolysaccharides) secreted by foraminifers (DeLaca and Lipps, 1972; Langer, 1993) acted both as cementing glue supporting the attachment to the skeletal fragment, as well as reactive organic matter available for bacteria proliferation (Graham and Cooper, 1959; Meyer-Reil and Köster, 1991; Richardson and Cedhagen; 2001). Moreover, pyrite framboids would have been a further agent stabilising foraminifers on the bioclast. Different survival strategies have been discussed for benthic foraminifers thriving in apparently unfavourable environments (e.g., symbiotic sulfur oxidizing bacteria, kleptoplastidy, peroxisome proliferation, commensalism; Bernhard and Buck, 2004; Bernhard and Bowser, 2008).

Considering all the above, low but persistent sedimentation rates should be invoked for the development of the analysed macroids. Similar environmental conditions influence growth rates of present-day reef and deeper-water macroids (Bassi et al., 2012, 2020). This setting would have inhibited formation of true hardground surfaces. Prolonged exposure of sea floor is known to promote mineralisation of substrates, thus providing a renewable supply of potassium, iron, and phosphate ions for the formation of glauconite and phosphate (Bromley, 1967; Kennedy and Garrison, 1975). Small amounts of glauconite and apatite, the former scattered in the siliciclastic matrix and the latter filling foraminifera chambers, indicate that mineralisation occurred throughout growth of the macroid pavements. Nevertheless, these minerals occur as minor constituents, indicating that strong glauconitisation and phosphatisation did not occur. The amount and kind of mineralisation suggest only ephemeral periods of reduced sedimentation or non-deposition. During these temporary submarine exposures, each nucleus of a future macroid acted as hard substrate, which was subsequently coated by pioneering encrusting foraminifers.

Episodic moderate to high energy events (i.e., storms), as well as bioturbation are invoked to explain both the complex arrangement of some foraminiferal encrustations and the distribution of bryozoans and serpulids on the external surfaces of macroids. Frequent overturns are considered as a necessary mechanism of nodule

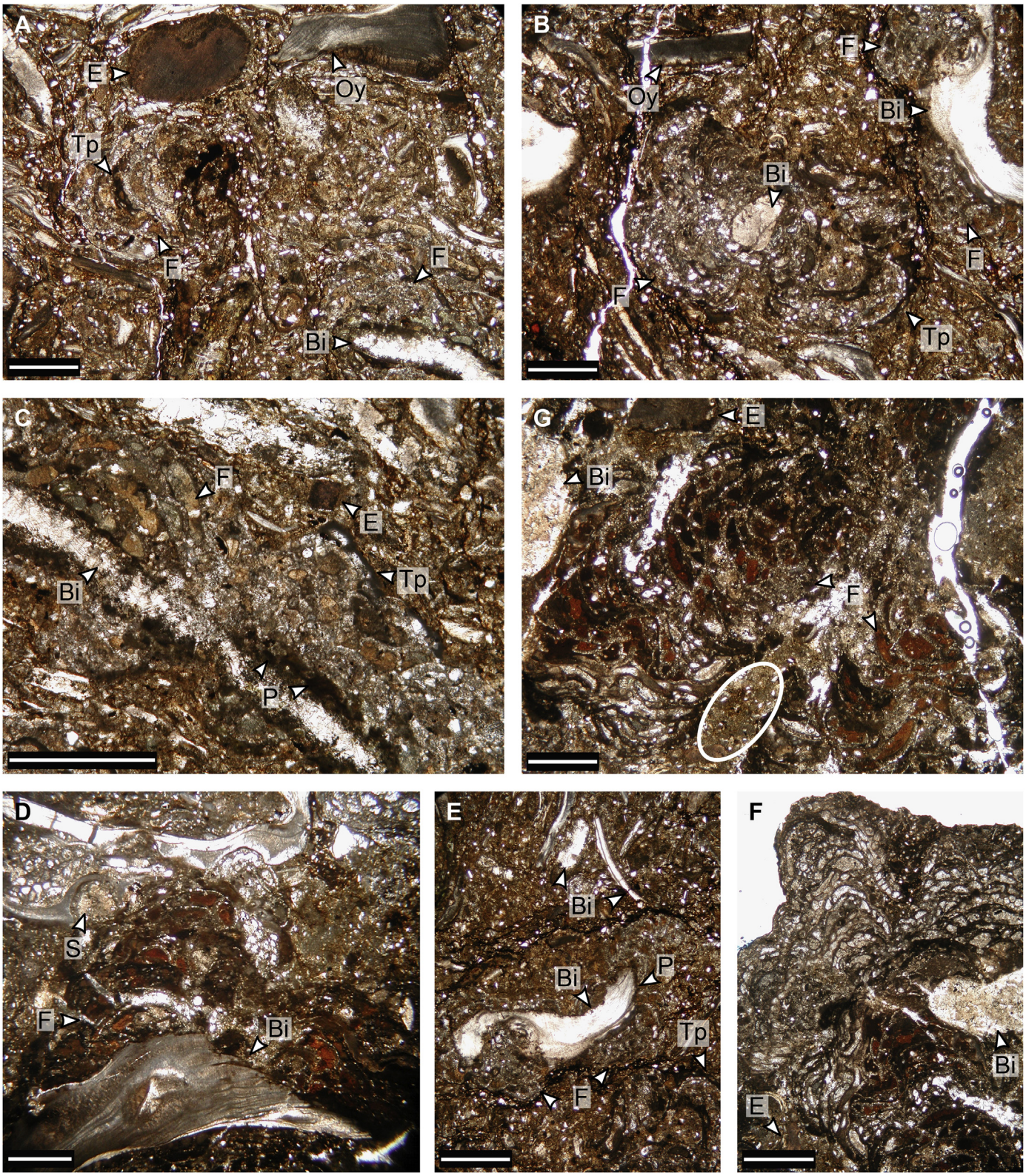


**Fig. 6.** Internal growth fabric of macroids. A, B, E) Agglutinated foraminifers encrusting the whole surface of skeletal nuclei. C) Detail of encrusting agglutinated foraminifers around a bioclastic nucleus. Note how the bioclast surface is coated by pyrite framboids at foraminiferal attachment surfaces. D) Encrusting agglutinated foraminifers showing the characteristic convex-upward growth reflecting the concavo-convex attachment surface of the skeletal nucleus they encrust. F) Gentle wavy morphology of foraminiferal tests with a fashion similar to small-scale stromatolitic structures. G) Foraminiferal chambers arranged in an irregular, sub-concentric manner; note overlap of the chambers, hampering recognition of isolated individuals. Circled area highlights an elongate depression separating foraminiferal growth stages infilled by fine-grained siliciclastic matrix rich in fine-bioclastic debris. F: foraminifer; Bi: bioclast; Oy: oyster; S: serpulid; E: echinoderm; Tp: ?*Tolypammina*; P: pyrite framboid. Scale bars = 1 mm.

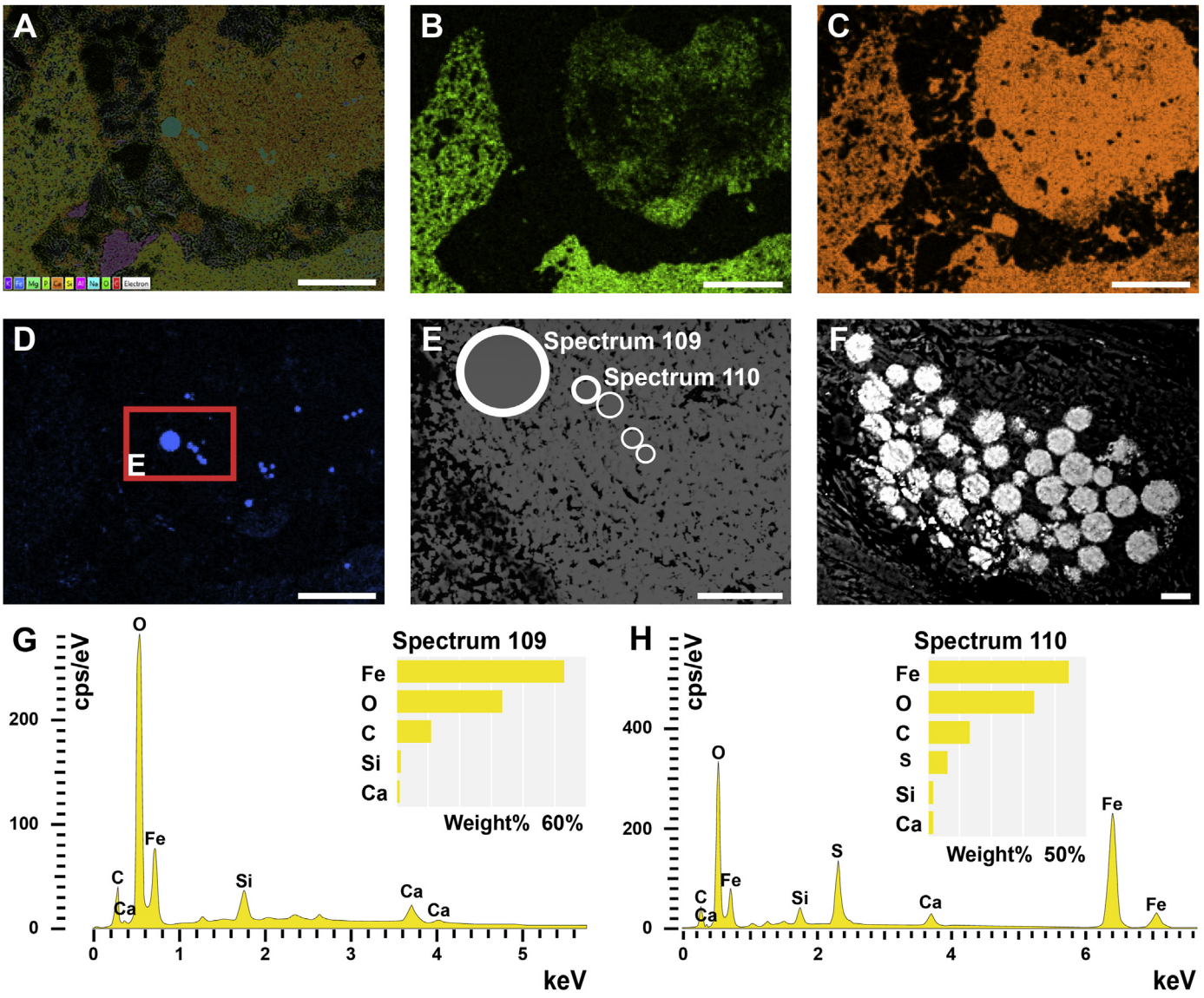


**Fig. 7.** SEM photomicrographs of pyrite framboids. A-D) EDX mappings showing framboidal pyrite in the interior of a foraminifer chamber. Apatite and calcite represent the filling minerals, as P and Ca dominate in the interior of the chamber (B, C). Scale bars = 100 μm. E) Detail of pyrite framboids of different sizes and related EDX spectra showing S and Fe concentrations. Scale bar = 25 μm. F) SEM image of a cluster of pyrite framboids of different sizes in the fine-grained siliciclastic matrix. Scale bar = 10 μm. G, H) EDX spectra of two framboids shown in (E), marked as Spectrum 109 and 110. Note that in the smaller framboids (Spectrum 110) Fe and S are preserved, whereas in the largest framboid (Spectrum 109) degradation of sulphur concentration is evident.

formation by different authors, who suggested a relationship between internal growth form and external shape of nodules (e.g., spherical shapes and concentric growths of coralline algae are interpreted as product of frequent waves or strong currents action) (Bosellini and Ginsburg, 1971; Bosence, 1983). However, biological activity by burrowing organisms or browsing fishes have also been considered responsible for nodule movements (e.g., Glynn, 1974; Pereira-Filho et al., 2015), thus favouring their growth in different directions resulting in sub-spheroidal morphologies. The foraminiferal growth fabrics observed in our macroids suggest modest overturning of the nodules, favouring the exposure of new surfaces available to be encrusted. A low magnitude of waves or currents affecting the sea floor can be inferred from lack of evidence of breakage of the foraminiferal encrustations. This coincides with the generally low-energy environment that lacks significant palaeoenvironmental fluctuations (i.e., changes in sedimentation rates, water chemistry). Bryozoan colonies are limited to the external surfaces of macroids, thus indicating that they did not actively participate in the formation of macroids, but represent a second encrustation event. However, these encrusting organisms were detected both on the upper and lower side of the nodules, which suggests overturning of the macroids thereby offering new hard surfaces to be encrusted. The environmental interpretation derived from macroid features fits well the interpretation proposed by Archuby and Fürsich (2010), who inferred an outer ramp (offshore) depositional environment for the facies containing macroids (Facies 5.2, allochemic mudrocks), based on sedimentological and taphonomic information.

### 5.1.2. *Oxygen levels*

Pyrite is a common constituent of ancient and modern, reducing marine sediments (Berner, 1970; Wilkin et al., 1996, 1997; Wignall and Newton, 1998; Wignall et al., 2005; Wei et al., 2012), either as inorganic sedimentary pyrite (e.g., Graham and Ohmoto, 1994; Ohfuji and Rickard, 2005) or as biogeochemical pyrite. In marine sedimentary environments with organic matter on the sea-floor,

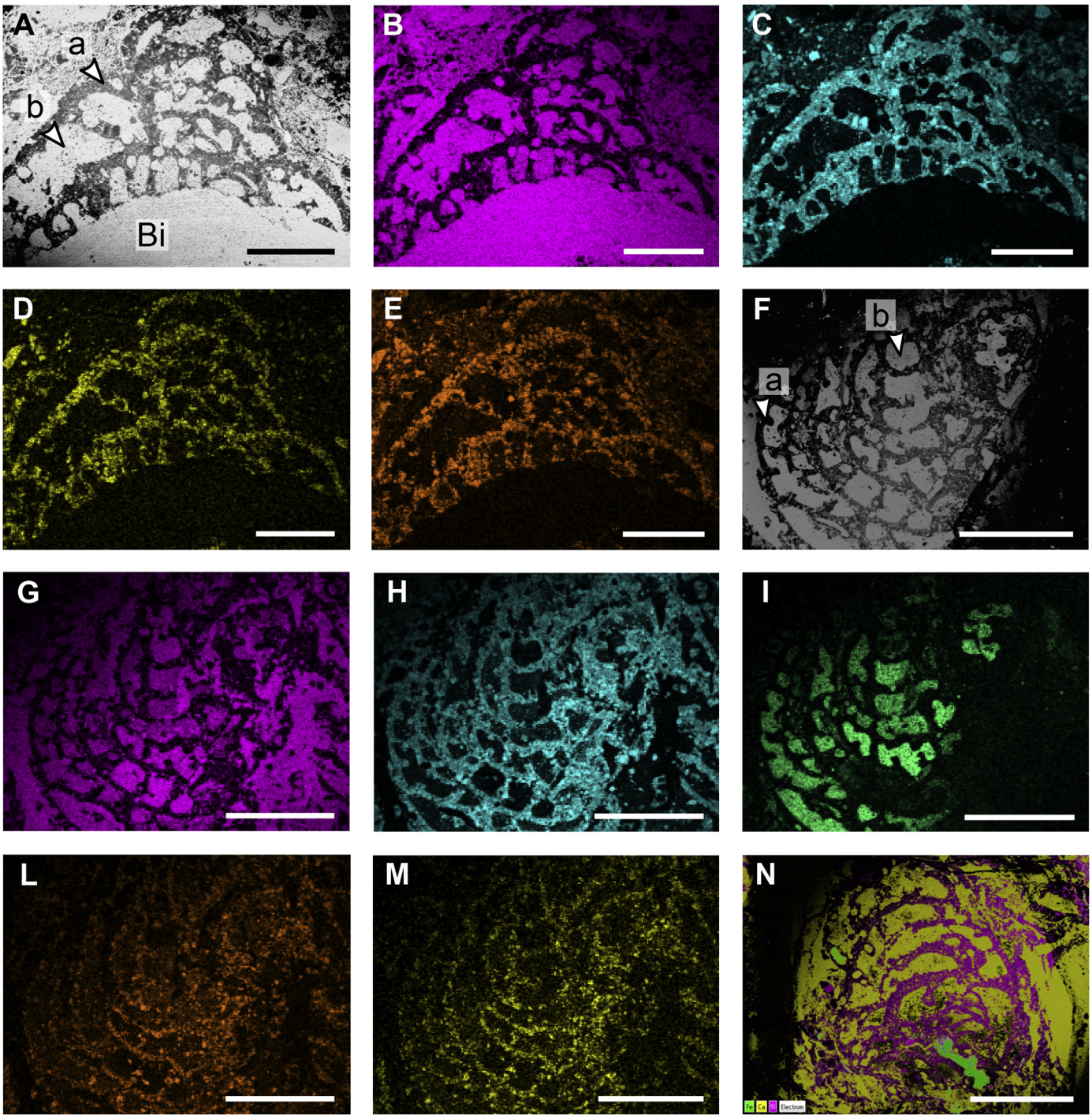


**Fig. 8.** SEM images and element mapping images of foraminifera chambers and tests (Ca, P, Si, Na, Al). A-E) Encrusting foraminifera with convex-upward growth showing that Ca dominates the interior of the chambers and Si, Na and Al constitute the test. (A) shows a SEM image of the foraminiferal specimen, while (B) to (E) correspond to element mapping images. Scale bars = 500 μm. F-M) Strongly curved morphology of encrusting foraminifera with Ca and P as main elements filling the chambers, and Si, Na, and Al constituting the test. (F) shows a SEM image of the foraminiferal specimen, whereas (G) to (M) correspond to element mapping images. Scale bars = 1 mm. N) EDX mapping showing Si as main constituent of the foraminiferal tests, and Ca and Fe as principal components of the chamber fills. Scale bar = 1 mm. Bi: bioclast; a: foraminiferal test; b: foraminifera chamber.

sulfate-reducing bacteria generate microcrystal aggregates commonly clustered in typical spherical framboids (e.g., Berner, 1970; Wilkin and Barnes, 1997; Folk, 2005; Merinero et al., 2010; Wei et al., 2012). Size distribution of framboidal pyrite in modern sedimentary settings has been used to reconstruct the redox conditions at ancient marine sea floors (Wilkin et al., 1996, 1997; Wilkin and Barnes, 1997). Framboidal pyrite growing close to the redox boundary, where concentration of sulfur-reducing bacteria is much higher, acquires the largest average sizes and a wider size range (e.g., Merinero et al., 2010). Pyrite framboids from the Agua de la Mula Member range from 2.5 μm to 25 μm in size, suggesting that the sediment-water interface of the upper Hauterivian beds studied falls into the upper dysoxic zone. If oxygen restrictions existed, they likely persisted below the sediment-water interface,

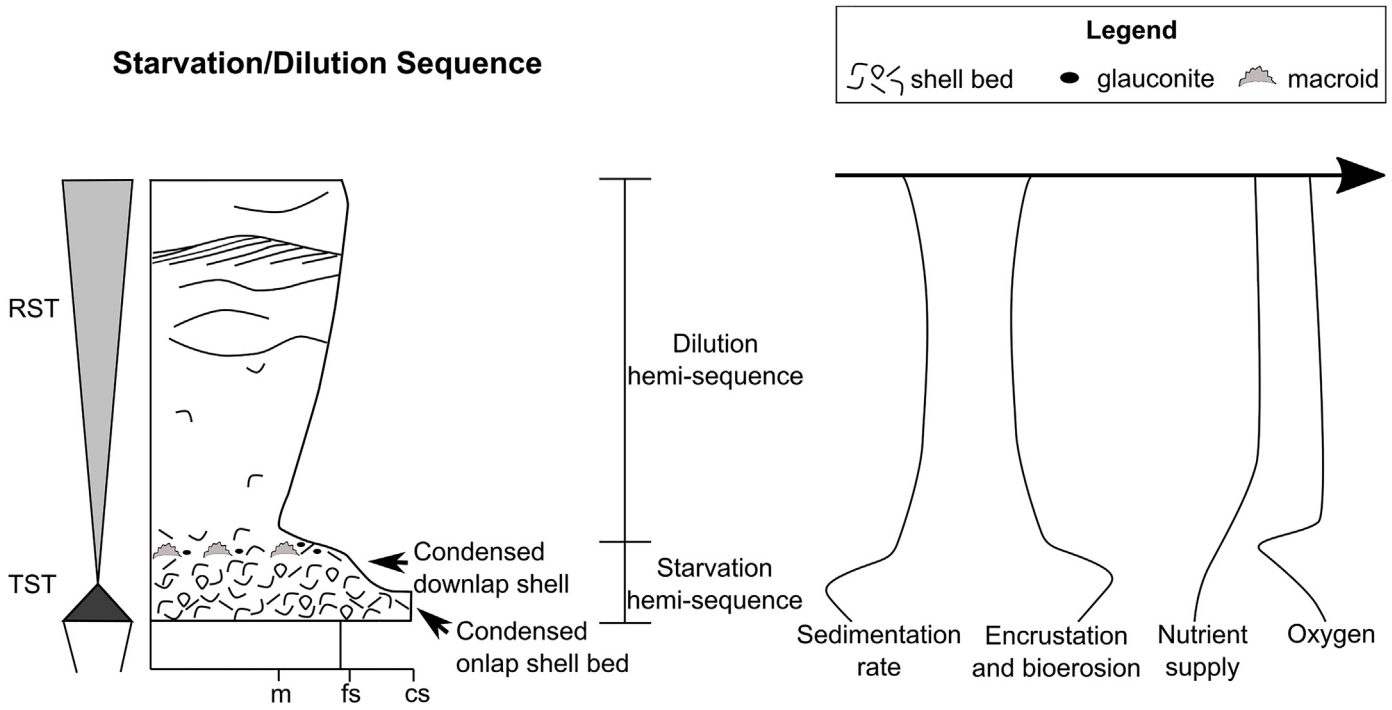


**Fig. 9.** Schematic model of starvation-dilution sequences (not to scale) and position of condensed shell beds (for further detail see Archuby and Fürsich, 2010). Condensed onlap shell beds rest on sharp or even erosional surfaces. Condensed downlap shell beds developed in the early phase of the next regression. Interpretations of sedimentation rate, encrustation and bioerosion, nutrient supply, and oxygen are schematic. TST: Transgressive systems tract; RST: Regressive systems tract; m: mud; fs: fine-grained sandstone; cs: coarse-grained sandstone.

while the oxygen content increased upward from the sediment-water interface throughout the water column. The benthic macrofauna in the beds containing macroids suggests also that there was no permanent oxygen depletion. A similar interpretation has been also proposed by Comerio et al. (2018, 2020) for the lowermost part of the Agua de la Mula Member. However, temporal (seasonal?) anoxia above the sediment-water interface cannot be discarded.

#### 5.1.3. Trophism

Mechanisms controlling accumulation of organic matter in marine sediments are still debated (e.g., Tyson and Pearson, 1991; Arthur and Sageman, 1994; Loubere and Fariduddin, 1999; Tyson et al., 2005). Organic matter accumulates when organisms are not able to consume it completely, either due to high rates of production, lowered rates of consumption (usually linked to deficiencies of oxygen) or both. We infer that pulses of continental runoff associated with increased terrigenous sedimentation rates provided nutrients to the basin. High levels of nutrients affect the sedimentary environment with consequent effects on the composition of macro- and microfaunal assemblages and on the depth of the photic zone, i.e. increased turbidity of the water column (Lukasik et al., 2000).

Infaunal/epifaunal ratio informs on the niche distribution of foraminifers and temporal (seasonal) anoxia mentioned above. The ratio can be indirectly related to oxygen levels and food availability (e.g., Corliss and Chen, 1988; Bernhard, 1989; Carson et al., 2008). Under eutrophic conditions oxygen is the main factor controlling the depth of infaunal foraminifera, while under more oligotrophic conditions the microfaunal distribution is mainly food-controlled (Jorissen et al., 1995). Thus, when eutrophic environments are highly oxygen-stressed, infaunal niches become smaller and foraminifera occupy shallower depths and when critical oxygen levels affect the deeper sediment layers infaunal taxa can live at the sediment-water interface (Jorissen et al., 1995). At the same time, less oxygen-tolerant epifaunal taxa will be at a disadvantage and their niche will be occupied by infaunal taxa. Nevertheless, in certain cases, opportunistic epifaunal species are pioneer taxa able to colonise the sediment-water interface under oxygen-poor conditions (e.g., Barmawidjaja et al., 1992; Jorissen et al., 1995). Taking this into account, the prevalence of encrusting foraminifers forming macroids and the relative scarcity of infaunal foraminifers suggests that benthic life persisted only at the sediment-water interface where the water column was not highly oxygen-depleted (upper dysoxic), thus promoting the growth of epifauna. In this scenario, the coating settler community is composed of opportunistic epifauna, living under most likely eutrophic conditions. Moreover, the type of sediment did not favour a thriving infauna as macroid formation preceded re-establishment of sediment input, which blanketed the substrate with mud (see next section).

### 5.2. Macroids and sequence stratigraphy

Knobby pavements and dome-like deposits made of macroids are sandwiched between coarse-grained mixed carbonate and siliciclastic beds and grey/dark pelitic and marly clay packages at the top of terrigenous starved beds of high-frequency sequences. Macroids are less common in the BAL section than in the AM section and, as indicated by Archuby and Fürsich (2010), occur in the latest Hauterivian *C. diamantensis* Zone within the third 3rd-order transgressive systems tract (Fig. 2). Starvation/dilution (S/D) sequences refer to couplets packages interpreted as eustatic 6th-order Milankovitch precession-driven cycles (Archuby and Fürsich, 2010; Archuby et al., 2011). Starvation hemi-sequences consist of thin, tabular beds, deepening upward with very dense skeletal concentrations, while dilution hemi-sequences consist of thicker siliciclastic-dominated beds, coarsening- and shallowing-upward with rare faunal remains. S/D sequences are developed throughout most of the Agua de la Mula Member following the

overall deepening and shallowing trend of the basin (for the position of S/D sequences within the transgressive-regressive systems tracts see Archuby and Fürsich, 2010). Key surfaces cannot always be detected in these (few to sub-) metre-scale packages. These couplets are relatively thin compared to higher hierarchy (3rd- or 4th-order) sequences, which makes it harder to interpret them (Lukasik and James, 2003; Archuby et al., 2011). Each S/D sedimentary cycle records changes in the sedimentation rate, carbonate availability and accommodation space, illustrating an environmental shift from the outer ramp (offshore zone) to the inner-proximal ramp (lower shoreface). Macroids occur invariably at the top of complex starvation deposits of the S/D sequences. Starvation hemi-sequences containing macroids comprise, from base to top, a coarse-grained mixed sandy-and bioclastic bed, inferred to have been deposited on the inner to middle ramp (probably including elements eroded from the preceding sequence, i.e. a lag deposit); a fining-upward trend with evidence of maximum starvation at the top; and a bed with abundant bioclasts embedded in a fine siliciclastic matrix. The base of starvation hemi-sequences is often erosional and contains a macrofauna rich in large mollusc shells affected by fair-weather processes and/or frequent storm waves. These transgressive lag deposits are interpreted as equivalent to condensed onlap shell beds *sensu* Kidwell (1991), Kondo et al. (1998), and Archuby (2009), deposited during the early 6th-order transgression. Without any sharp boundary, these early starvation beds grade to the lower-energy (with well-preserved fauna), high diversity middle starvation hemi-sequence, characterised by intense bioerosion and encrustation, inferred as the maximum flooding level (Archuby, 2009). The last shell rich layer is usually poorly recorded and/or amalgamated with the overlaying next regression beds. Although still starved, they are inferred to have been deposited during the early phase of the next regression. The preservation of faunal content is optimal in this package, with high degrees of articulation and scarce bioerosion (Archuby, 2009). These shell beds are inferred to correspond to the downlap condensed shell beds *sensu* Kidwell (1991), Kondo et al. (1998) and Archuby (2009). When macroids occur, they are located between the highly condensed maximum flooding level and the base of pelitic and marly-argillaceous dilution interval, always as part of the downlap condensed shell beds, characterised by moderate degree of starvation but associated with fine-grained terrigenous mud (Fig. 9).

During transgression, deposition of terrigenous sediment shifted landward following the receding shoreline (retrogradational pattern), thereby decreasing the nutrient content of the sea water, which became less eutrophic. Renewed sediment input after maximum flooding started with fine-grained sediments that contained nutrients from the hinterland (Archuby and Fürsich, 2010), which led to eutrophication of the water mass. The terrigenous input during dilution hemi-sequences increased the trophic resources and triggered a change in the character of the sea floor, from a mostly bioclastic substrate to a mosaic of soft and shelly patches (according to the record of benthic macrofossils), and finally to a homogeneous muddy sediment. High trophic resources inhibited carbonate production and decreased accumulation rates, favouring calcium carbonate dissolution (i.e., benthic macro- and microfauna found it harder to secrete calcareous tests) and, indirectly, destruction by bioerosion (Hallock, 1987, 1988; Lukasik et al., 2000; Lukasik and James, 2003; Archuby, 2009). An excess of organic matter production increased the demand of oxygen and, at the same time, reduced light-penetration as a consequence of increased turbidity. This in turn caused a reduction of photosynthesis, further reinforcing the oxygen stress. In an extreme case, the bottom community was restricted to a set of few species that took advantage of the high trophic resource level and were able to cope with reduced oxygen levels. Under these conditions, low-diversity communities dominated by opportunistic species flourished (Hallock, 1987). Also, formation of firmgrounds and hardgrounds coated with glauconite, phosphate, or iron oxide were promoted (Hallock, 1987; Lukasik et al., 2000). The initial colonization by both opportunistic foraminifers and filter feeding serpulids and oysters, marked the switch in the community to a typical eutrophic one. While the rate of sedimentation was still low, i.e. during relative sea-level stillstand when transgression changed to early regression, buildups formed and low-diversity communities developed. However, occasional excess of nutrients, combined with increased turbidity, consumed most of the oxygen, resulting in a high-stress environment for the benthic microfauna. Macroid-building foraminifers were promoted and colonized a hostile sea floor with plenty of organic matter but not suitable for competitors.

When zooming out stratigraphically, it becomes interesting that, although similar foraminifers are common encrusters of shells in middle to late starvation hemi-sequences, macroids only occurred during the latest Hauterivian 3rd-order transgression. Archuby et al. (2011) detected a possible analogue of the Faraoni Anoxic Event (Cecca et al., 1994) coinciding with the maximum flooding of the DSAM-3, just above the transgressive systems tract TST-3 that bears macroids. It seems that the latest Hauterivian transgression imposed particular conditions, probably a faster retrogradation, that created conditions for pulses of oxygen deficiencies in every high-frequency sequence and a stronger maximum flooding.

## 6. Conclusions

Macroid pavements and dome-like deposits, mainly composed of agglutinated encrusting foraminifers with convex-upward and circum-granular growths around skeletal nuclei, are outstanding features of some high-frequency cycles of the Agua de la Mula Member (Agrio Formation). These foraminiferal pavements occur as part of downlap condensed shell beds of 6th-order starvation/dilution (S/D) sequences, in terrigenous sediment-starved deposits. Although agglutinated encrusting foraminifers are widespread in middle to late starved beds of high-frequency cycles, macroids developed only in those deposited during the latest Hauterivian third 3rd-order transgressive systems tract. Palaeoecological and palaeoenvironmental analyses suggest that macroids were deposited after the restoration of terrigenous sediment input, but still under low sedimentation rates, in marine reduced conditions. The starved beds containing macroids passed through very low to high sedimentation rates, recorded by bioclastic condensed beds and pelitic and marly-argillaceous intervals, respectively. The re-establishment of terrigenous sediment input at the onset of the 6th-order regression triggered the development of a series of phenomena that culminated in an oxygen-stressed habitat: sedimentation introduced nutrients from the hinterland, thus increasing the trophic resource level, which promoted further increase in turbidity and consequently reduced the depth of the photic zone. Photosynthesis did not compensate the consumption of oxygen in this highly eutrophic environment. The sea floor was beyond the reach of waves that could have introduced oxygen and thus became depleted in oxygen. Evidence is the size range distribution of pyrite framboids, suggesting their formation in the upper dysoxic zone close to the sediment-water interface. Scattered mineralisations of glauconite and apatite are consistent with such reducing conditions. We infer that the comparatively fast 3rd-order transgression led to a greater water depth at the end of every high-frequency transgression. These palaeoenvironmental conditions persisted until sediment input filled accommodation space, after which higher-energy and more oxygenated conditions became

established. More generally, our study confirms that macroids are valuable tools for highly detailed palaeoecological and palaeoenvironmental reconstructions of high-frequency sequences in mixed siliciclastic-carbonate ramp systems.

## Acknowledgements

This research was supported by Universidad Nacional de Río Negro - Argentina (PI UNRN 2017 40-A-612 project). Paolo Citton and Damiano Palombi are warmly thanked for their support during the fieldwork. Diego Kietzmann, an anonymous reviewer, and the Editor-in-Chief Eduardo Koutsoukos are acknowledged for suggestions and constructive comments that improved the manuscript.

## References

Aguirre-Urreta, M.B., 1995. Nota Paleontológica. *Spitidiscus riccardii* Leanza y Wiedmann (Ammonoidea) en el Hauteriviano del Neuquén. Ameghiniana 32 (4), 407–410.

Aguirre-Urreta, M.B., Rawson, P.F., 1997. The ammonite sequence in the Agrio Formation (Lower Cretaceous), Neuquén Basin, Argentina. Geological Magazine 134 (4), 449–458.

Aguirre-Urreta, M.B., Rawson, P.F., Concheyro, G.A., Bown, P.R., Ottone, E.G., 2005. Lower Cretaceous (Berriasian-Aptian) biostratigraphy of the Neuquén Basin. In: Veiga, G.D., Spalletti, L.A., Howell, J.A., Schwarz, E. (Eds.), The Neuquén Basin: A case study in sequence stratigraphy and basin dynamics, Special Publications, vol. 252. The Geological Society, London, pp. 57–81.

Archuby, F.M., 2009. Taphonomy and palaeoecology of benthic macroinvertebrates from the Agua de la Mula Member of the Agrio Formation, Neuquén Basin (Neuquén province, Argentina): sequence stratigraphic significance. Ph.D. thesis. Universität Würzburg, Germany, p. 349.

Archuby, F.M., Fürsich, F.T., 2010. Facies analysis of a higly cyclic sedimentary unit: the Late Hauterivian to Early Barremian Agua de la Mula Member of the Agrio Formation, Neuquén Basin, Argentina. Beringeria 41, 77–127.

Archuby, F.M., Wilmsen, M., Leanza, H.A., 2011. Integrated stratigraphy of the Upper Hauterivian to Lower Barremian Agua de la Mula Member of the Agrio Formation, Neuquén Basin, Argentina. Acta Geologica Polonica 61 (1), 1–26.

Arthur, M.A., Sageman, B.B., 1994. Marine black shales: depositional mechanisms and environments of ancient deposits. Annual Review of Earth and Planetary Sciences 22 (1), 499–551.

Ballent, S., Concheyro, A., Sagasti, G., 2006. Bioestratigrafía y paleoambiente de la Formación Agrio (Cretácico Inferior), en la Provincia de Mendoza, Cuenca Neuquina, Argentina. Revista Geologica de Chile 33 (1), 47–79.

Barmawidjaja, D.M., Jorissen, F.J., Puskaric, S.V., Van der Zwaan, G.J., 1992. Microhabitat selection by benthic foraminifera in the northern Adriatic Sea. Journal of Foraminiferal Research 22 (4), 297–317. https://doi.org/10.2113/gsjfr.22.4.297.

Bassi, D., Braga, J.C., Owada, M., Aguirre, J., Lipps, J.H., Takayanagi, H., Iryu, Y., 2020. Boring bivalve traces in modern reef and deeper-water macroid and rhodolith beds. Progress in Earth and Planetary Science 7 (1), 1–17. https://doi.org/10.1186/s40645-020-00356-w.

Bassi, D., Iryu, Y., Humblet, M., Matsuda, H., Machiyama, H., Sasaki, K., Matsuda, S., Arai, K., Inoue, T., 2012. Recent macroids on the Kikai-jima shelf, Central Ryukyu Islands, Japan. Sedimentology 59 (7), 2024–2041. https://doi.org/10.1111/j.1365-3091.2012.01333.x.

Berner, R.A., 1970. Sedimentary pyrite formation. American Journal of Science 268 (1), 1–23. https://doi.org/10.2475/ajs.268.1.1.

Berner, R.A., 1984. Sedimentary pyrite formation: an update. Geochimica et Cosmochimica Acta 48 (4), 605–615. https://doi.org/10.1016/0016-7037(84)90089-9.

Bernhard, J.M., 1989. The distribution of benthic Foraminifera with respect to oxygen concentration and organic carbon levels in shallow-water Antarctic sediments. Limnology & Oceanography 34 (6), 1131–1141. https://doi.org/10.4319/lo.1989.34.6.1131.

Bernhard, J.M., Bowser, S.S., 2008. Peroxisome proliferation in Foraminifera inhabiting the chemocline: An adaptation to reactive oxygen species exposure? The Journal of Eukaryotic Microbiology 55 (3), 135–144. https://doi.org/10.1111/j.1550-7408.2008.00318.x.

Bernhard, J.M., Buck, K.R., 2004. Eukaryotes of the Cariaco, Soledad, and Santa Barbara Basins: protists and metazoans associated with deep-water marine sulfide-oxidizing microbial mats and their possible effects on the geologic record. In: Amend, J.P., Edwards, K.J., Lyons, T.W. (Eds.), Sulfur Biogeochemistry – Past and Present, Special paper, vol. 379. Geological Society of America, pp. 35–48.

Bosellini, A., Ginsburg, R.N., 1971. Form and internal structure of Recent algal nodules (rhodolites) from Bermuda. The Journal of Geology 79 (6), 669–682. https://doi.org/10.1086/627697.

Bosellini, F.R., Papazzoni, C.A., 2003. Palaeoecological significance of coral-encrusting foraminiferan associations: A case-study from the Upper Eocene of northern Italy. Acta Palaeontologica Polonica 48 (2), 279–292.

Bosence, D.W., 1983. Description and classification of rhodoliths (rhodoids, rhodolites). In: Peryt, T.M. (Ed.), Coated grains. Springer, Berlin, Heidelberg, pp. 217–224. https://doi.org/10.1007/978-3-642-68869-0_19.

Brett, C.E., Allison, P.A., 1998. Paleontological approaches to the environmental interpretation of marine mudrocks. In: Schieber, J., Zimmerle, W., Sethi, P.S. (Eds.), Shales and Mudstones (Volume I, Basin studies, sedimentology, and paleontology). Schweizerbart, Stuttgart, Germany, pp. 301–349.

Bromley, R.G., 1967. Marine phosphorites as depth indicators. Marine Geology 5 (5–6), 503–509. https://doi.org/10.1016/0025-3227(67)90057-6.

Carson, B.E., Francis, J.M., Leckie, R.M., Droxler, A.W., Dickens, G.R., Jorry, S.J., Bentley, S.J., Peterson, L.C., Opdyke, B.N., 2008. Benthic foraminiferal response to sea level change in the mixed siliciclastic-carbonate system of southern Ashmore Trough (Gulf of Papua). Journal of Geophysical Research 113, F01S20. https://doi.org/10.1029/2006JF000629.

Carter, H.J., 1877. Description of *Bdelloidina aggregata*, a new genus and species of arenaceous foraminifera, in which their so-called "Imperforation" is questioned. Annals and Magazine of Natural History 19 (111), 201–209. https://www.biodiversitylibrary.org/page/26456828atalov.

Čatalov, G.A., 1983. Triassic oncoids from central Balkanides (Bulgaria). In: Peryt, T.M. (Ed.), Coated grains. Springer, Berlin, Heidelberg, pp. 398–408. https://doi.org/10.1007/978-3-642-68869-0_35.

Cecca, F., Marini, A., Pallini, G., Baudin, F., Begouen, V., 1994. A guide-level of the uppermost Hauterivian (Lower Cretaceous) in the pelagic succession of Umbria-Marche Apennines (Central Italy): the Faraoni Level. Rivista Italiana di Paleontologia e Stratigrafia 99 (1993), 551–568.

Chapman, F., 1898. On *Haddonia*, a new genus of the foraminifera, from Torres Straits. Zoological Journal of the Linnean Society 26 (169), 452–456.

Comerio, M., Fernández, D.E., Pazos, P.J., 2018. Sedimentological and ichnological characterization of muddy storm related deposits: the upper Hauterivian ramp of the Agrio Formation in the Neuquén Basin, Argentina. Cretaceous Research 85, 78–94. https://doi.org/10.1016/j.cretres.2017.11.024.

Comerio, M., Fernández, D.E., Gutiérrez, C., Justiniano, C.B., Estebenet, M.C.G., Pazos, P.J., 2019. Sedimentary evolution of the marine Agua de la Mula Member (Agrio Formation, Lower Cretaceous) in the central Neuquén Basin: source areas and paleogeographic considerations from a distal setting. Journal of South American Earth Sciences 96, 102259. https://doi.org/10.1016/j.jsames.2019.102259.

Comerio, M., Fernández, D.E., Rendtorff, N., Cipollone, M., Zalba, P.E., Pazos, P.J., 2020. Depositional and postdepositional processes of an oil-shale analog at the microstructure scale: the Lower Cretaceous Agrio Formation, Neuquén Basin, northern Patagonia. AAPG Bulletin 104 (8), 1679–1705. https://doi.org/10.1306/04082017419.

Corliss, B.H., Chen, C., 1988. Morphotype patterns of Norwegian Sea deep-sea benthic foraminifera and ecological implications. Geology 16 (8), 716–719. https://doi.org/10.1130/0091-7613(1988)016<0716:MPONSD>2.3.CO;2.

Delaca, T.E., Lipps, J.H., 1972. The mechanism and adaptive significance of attachment and substrate pitting in the foraminiferan *Rosalina globularis* d'Orbigny. Journal of Foraminiferal Research 2 (2), 68–72. https://doi.org/10.2113/gsjfr.2.2.68.

Denayer, J., 2018. From rolling stones to rolling reefs: a Devonian example of highly diverse macroids. Lethaia 51 (4), 564–580. https://doi.org/10.1111/let.12278.

Dugolinsky, B.K., Margolis, S.V., Dudley, W.C., 1977. Biogenic influence on growth of manganese nodules. Journal of Sedimentary Research 47 (1), 428–445. https://doi.org/10.1306/212F7194-2B24-11D7-8648000102C1865D.

Flugel, E., 1967. Eine neue foraminifere aus den Riff kalken der nord alpinen Ober Trias: *Alpinophragmium perforatum* n. gen n. sp. Senck Lethaea 48 (5), 318–402.

Flügel, E., 2004. Microfacies of carbonate rocks: analysis, interpretation and application. Springer Science & Business Media.

Folk, R.L., 2005. Nannobacteria and the formation of framboidal pyrite: Textural evidence. Journal of Earth System Science 114 (3), 369–374. https://doi.org/10.1007/BF02702955.

Fürsich, F.T., Pandey, D.K., 2003. Sequence stratigraphic significance of sedimentary cycles and shell concentrations in the Upper Jurassic – Lower Cretaceous of Kachchh, western India. Palaeogeography, Palaeoclimatology, Palaeoecology 193, 149–159. https://doi.org/10.1016/S0031-0182(03)00233-5.

Fürsich, F.T., Oschmann, W., Singh, I.B., Jaitly, A.K., 1992. Hardgrounds, reworked concretion levels and condensed horizons in the Jurassic of western India: their significance for basin analysis. Journal of the Geological Society London 149 (3), 313–331. https://doi.org/10.1144/gsjgs.149.3.0313.

Gischler, E., Ginsburg, R.N., 1996. Cavity dwellers (coelobites) under coral rubble in southern Belize barrier and atoll reefs. Bulletin of Marine Science 58 (2), 570–589.

Glynn, P.W., 1974. Rolling stones among the Scleractinia: mobile corralliths in the Gulf of Panama. In: Proceedings of the 2nd International Coral Reef Symposium, Brisbane, vol. 2, pp. 183–198.

Graham, J.W., Cooper, S.C., 1959. Biological origin of manganese-rich deposits of the sea floor. Nature 183 (4667), 1050–1051. https://doi.org/10.1038/1831050a0.

Graham, U.M., Ohmoto, H., 1994. Experimental study of formation mechanisms of hydrothermal pyrite. Geochimica et Cosmochimica Acta 58 (10), 2187–2202. https://doi.org/10.1016/0016-7037(94)90004-3.

Greenslate, J., 1974. Microorganisms participate in the construction of manganese nodules. Nature 249 (5453), 181–183.

Guler, M.V., Lazo, D.G., Pazos, P.J., Borel, C.M., Ottone, E.G., Tyson, R.V., Cesaretti, N., Aguirre-Urreta, M.B., 2013. Palynofacies analysis and palynology of the Agua de la Mula Member (Agrio Formation) in a sequence stratigraphy framework,

Lower Cretaceous, Neuquén Basin, Argentina. Cretaceous Research 41, 65–81. https://doi.org/10.1016/j.cretres.2012.10.006.
Hallock, P., 1987. Fluctuations in the trophic resource continuum: a factor in global diversity cycles? Paleoceanography 2 (5), 457–471. https://doi.org/10.1029/PA002i005p00457.
Hallock, P., 1988. The role of nutrient availability in bioerosion: consequences to carbonate buildups. Palaeogeography, Palaeoclimatology, Palaeoecology 63 (1–3), 275–291. https://doi.org/10.1016/0031-0182(88)90100-9.
Hedley, R.H., 1963. Cement and iron in the arenaceous foraminifera. Micropaleontology 9 (4), 433–441.
Hornung, T., Spatzenegger, A., Joachimski, M.M., 2007. Multistratigraphy of condensed ammonoid beds of the Rappoltstein (Berchtesgaden, southern Germany): unravelling palaeoenvironmental conditions on 'Hallstatt deep swells' during the Reingraben Event (Late Lower Carnian). Facies 53 (2), 267–292. https://doi.org/10.1007/s10347-006-0101-1.
Hottinger, L., 1983. Neritic macroid genesis, an ecological approach. In: Peryt, T.M. (Ed.), Coated grains. Springer, Berlin, Heidelberg, pp. 38–55. https://doi.org/10.1007/978-3-642-68869-0_5.
Howell, J.A., Schwarz, E., Spalletti, L.A., Veiga, G.D., 2005. The Neuquén Basin: an overview. In: Veiga, G.D., Spalletti, L.A., Howell, J.A., Schwarz, E. (Eds.), The Neuquén Basin, Argentina: a case study in sequence stratigraphy and basin dynamics, Special Publications, vol. 252. Geological Society, London, pp. 1–14.
Jenkyns, H.C., 1970. Fossil manganese nodules from the west Sicilian Jurassic. Eclogae Geologicae Helvetiae 63 (3), 741–774.
Johnson, J.H., 1946. Lime-secreting algae from the Pennsylvanian and Permian of Kansas. The Geological Society of America Bulletin 57 (12), 1087–1120. https://doi.org/10.1130/0016-7606(1946)57[1087:LAFTPA]2.0.CO;2.
Jones, B., Hunter, I.G., 1995. Vermetid buildups from Grand Cayman, British West Indies. Journal of Coastal Research 973–983. https://www.jstor.org/stable/4298404.
Jorissen, F.J., de Stigter, H.C., Widmark, J.G., 1995. A conceptual model explaining benthic foraminiferal microhabitats. Marine Micropaleontology 26 (1–4), 3–15. https://doi.org/10.1016/0377-8398(95)00047-X.
Kennedy, W.J., Garrison, R.E., 1975. Morphology and genesis of nodular chalks and hardgrounds in the Upper Cretaceous of southern England. Sedimentology 22 (3), 311–386. https://doi.org/10.1111/j.1365-3091.1975.tb01637.x.
Kidwell, S.M., 1991. Condensed deposits in siliciclastic sequences: expected and observed features. In: Einsele, G., Ricken, W., Seilacher, A. (Eds.), Cycles and events in Stratigraphy. Springer-Verlag, Berlin, pp. 682–695.
Kidwell, S.M., Jablonski, D., 1983. Taphonomic feedback. Ecological consequences of shell accumulation. In: Tevesz, M.J.S., McCall, P.L. (Eds.), Biotic Interactions in Recent and Fossil Benthic Communities. Plenum, New York, pp. 195–248. https://doi.org/10.1007/978-1-4757-0740-3_5.
Kietzmann, D.A., Paulin, S.M., 2019. Cyclostratigraphy of an upper Valanginian–lower Hauterivian mixed siliciclastic-carbonate ramp succession (Pilmatué Member of the Agrio Formation), Loma La Torre section, northern Neuquén Basin, Argentina. Cretaceous Research 98, 26–46. https://doi.org/10.1016/j.cretres.2019.01.020.
Kondo, Y., Abbott, S.T., Kitamura, A., Kamp, P.J., Naish, T.R., Kamataki, T., Saul, G.S., 1998. The relationship between shellbed type and sequence architecture: examples from Japan and New Zealand. Sedimentary Geology 122 (1–4), 109–127. https://doi.org/10.1016/S0037-0738(98)00101-8.
Langer, M.R., 1993. Epiphytic foraminifera. Marine Micropaleontology 20 (3–4), 235–265. https://doi.org/10.1016/0377-8398(93)90035-V.
Leanza, H.A., Hugo, C.A., Repol, D., Gonzalez, R., Danieli, J.C., 2001. Hoja geológica 3969-I, Zapala, provincia del Neuquén. Instituto de Geología y Recursos Minerales–El Servicio Geológico Minero Argentino Boletín, 275, scale 1: 250,000.
Legarreta, L., Gulisano, C.A., 1989. Análisis estratigráfico secuencial de la Cuenca Neuquina (Triásico superior-Terciario inferior), Argentina. In: Chebli, G.A., Spalletti, L.A. (Eds.), Cuencas Sedimentarias Argentinas, Simp. Cuencas Sedimentarias Argentinas, Ser. Correlación Geol, vol. 6. Universidad Nacional de Tucuman, INSUGEO, Tucuman, pp. 221–244.
Legarreta, L., Uliana, M.A., 1991. Jurassic-Cretaceous marine oscillations and geometry of backarc basin fill, central Argentine Andes. In: Macdonald, D.I. (Ed.), Sedimentation, tectonics and eustasy. Sea level changes at active plate margins, Special Publication, vol. 12. International Association of Sedimentology, London, pp. 429–450.
Leiter, C., Altenbach, A.V., 2010. Benthic foraminifera from the diatomaceous mud belt off Namibia: characteristic species for severe anoxia. Palaeontologia Electronica 13 (2), 19.
Loubere, P., Fariduddin, M., 1999. Benthic foraminifera and the flux of organic carbon to the seabed. In: Sen Gupta, B.K. (Ed.), Modern foraminifera. Springer, Dordrecht, pp. 181–199.
Love, L.G., 1971. Early diagenetic polyframboidal pyrite, primary and redeposited, from the Wenlockian Denbigh Grit Group, Conway, North Wales, UK. Journal of Sedimentary Research 41 (4), 1038–1044. https://doi.org/10.1306/74D723EC-2B21-11D7-8648000102C1865D.
Love, L.G., Murray, J.W., 1963. Biogenic pyrite in Recent sediments of Christchurch Harbour, England. American Journal of Science 261 (5), 433–448. https://doi.org/10.2475/ajs.261.5.433.
Luci, L., Cichowolski, M., 2014. Encrustation in nautilids: a case study in the Cretaceous species *Cymatoceras perstriatum*, Neuquén Basin, Argentina. PALAIOS 29 (3), 101–120. https://doi.org/10.2110/palo.2013.062.
Lukasik, J.J., James, N.P., 2003. Deepening-upward subtidal cycles, Murray basin, South Australia. Journal of Sedimentary Research 73 (5), 653–671. https://doi.org/10.1306/031003730653.
Lukasik, J.J., James, N.P., McGowran, B., Bone, Y., 2000. An epeiric ramp: low-energy, cool-water carbonate facies in a Tertiary inland sea, Murray Basin, South Australia. Sedimentology 47 (4), 851–881. https://doi.org/10.1046/j.1365-3091.2000.00328.x.
Meyer-Reil, L.A., Köster, M., 1991. Fine-scale distribution of hydrolytic activity associated with foraminiferans and bacteria in deep-sea sediments of the Norwegian-Greenland Sea. Kiel Meeresforsch (Sonderh) 8, 121–126.
Merinero Palomares, R., Lunar Hernández, R., Somoza, L., Díaz-del-Río, V., Martínez-Frías, J., 2009. Nucleation, growth and oxidation of framboidal pyrite associated with hydrocarbon-derived submarine chimneys: lessons learned from the Gulf of Cadiz. European Journal of Mineralogy 21 (5), 947–961. https://doi.org/10.1127/0935-1221/2009/0021-1956.
Merinero Palomares, R., Lunar Hernández, R., Martínez-Frías, J., 2010. Carbonatos metanógenos y pirita framboidal autigénica: geomarcadores de la actividad de organismos quimiosintéticos en el Golfo de Cádiz. Macla 12, 29–37.
Mullineaux, L.S., 1988. Taxonomic notes on large agglutinated foraminifers encrusting manganese nodules, including the description of a new genus, *Chondrodapis* (Komokiacea). Journal of Foraminiferal Research 18 (1), 46–53. https://doi.org/10.2113/gsjfr.18.1.46.
Ohfuji, H., Rickard, D., 2005. Experimental syntheses of framboids—a review. Earth-Science Reviews 71 (3–4), 147–170. https://doi.org/10.1016/j.earscirev.2005.02.001.
Pattan, J.N., 1993. Manganese micronodules: a possible indicator of sedimentary environments. Marine Geology 113 (3–4), 331–344. https://doi.org/10.1016/0025-3227(93)90026-R.
Pereira-Filho, G.H., de Cerqueira Veras, P., Francini-Filho, R.B., de Moura, R.L., Pinheiro, H.T., Gibran, F.Z., Matheus, Z., Neves, L.M., Amado-Filho, G.M., 2015. Effects of the sand tilefish *Malacanthus plumieri* on the structure and dynamics of a rhodolith bed in the Fernando de Noronha Archipelago, tropical West Atlantic. Marine Ecology Progress Series 541, 65–73. https://doi.org/10.3354/meps11569.
Peryt, T.M., 1983. Classification of coated grains. In: Peryt, T.M. (Ed.), Coated grains. Springer, Berlin, Heidelberg, pp. 3–6. https://doi.org/10.1007/978-3-642-68869-0_1.
Perrin, C., 1992. Signification écologique des foraminifères acervulinidés et leur rôle dans la formation de faciès récifaux et organogènes depuis le Paléocène. Geobios-Lyon 25 (6), 725–751. https://doi.org/10.1016/S0016-6995(92)80054-H.
Pollastro, R.M., 1981. Authigenic kaolinite and associated pyrite in chalk of the Cretaceous Niobrara Formation, eastern Colorado. Journal of Sedimentary Research 51 (2), 553–562. https://doi.org/10.1306/212F7CD4-2B24-11D7-8648000102C1865D.
Prager, E.J., Ginsberg, R.N., 1989. Carbonate nodule growth on Florida's outer shelf and its implications for fossil interpretations. PALAIOS 4 (4), 310–312. https://doi.org/10.2307/3514555.
Reid, R.P., Macintyre, I.G., 1988. Foraminiferal-algal nodules from the eastern Caribbean; growth history and implications on the value of nodules as paleoenvironmental indicators. PALAIOS 3 (4), 424–435. https://doi.org/10.2307/3514788.
Resig, J.M., Glenn, C.R., 1997. Foraminifera encrusting phosphoritic hardgrounds of the Peruvian upwelling zone: taxonomy, geochemistry, and distribution. Journal of Foraminiferal Research 27, 133–150. https://doi.org/10.2113/gsjfr.27.2.133.
Richardson, K., Cedhagen, T., 2001. Quantifying pelagic-benthic coupling in the North Sea: are we asking the right questions? Senckenbergiana maritima 31, 215–224. https://doi.org/10.1007/BF03043030.
Richardson-White, S., Walker, S.E., 2011. Diversity, taphonomy and behavior of encrusting foraminifera on experimental shells deployed along a shelf-to-slope bathymetric gradient, Lee Stocking Island, Bahamas. Palaeogeography, Palaeoclimatology, Palaeoecology 312 (3–4), 305–324. https://doi.org/10.1016/j.palaeo.2011.02.021.
Rodríguez-Martínez, M., Heim, C., Simon, K., Zilla, T., Reitner, J., 2011. *Tolypammina gregaria* Wendt 1969-Frutexites assemblage and ferromanganese crusts: a coupled nutrient-metal interplay in the Carnian sedimentary condensed record of Hallstatt facies (Austria). In: Reitner, J., Queric, N.-V., Arp, G. (Eds.), Advances in Stromatolite Geobiology. Lecture Notes in Earth Sciences, vol. 131, pp. 409–434. https://doi.org/10.1007/978-3-642-10415-2_25.
Sagasti, G., 2000. La sucesión rítmica de la Formación Agrio (Cretácico inferior) en el sur de la provincia de Mendoza, y su posible vinculación con Ciclos de Milankovitch. Latin American Journal of Sedimentology and Basin Analysis 7 (1–2), 1–22.
Sagasti, G., 2005. Hemipelagic record of orbitally-induced dilution cycles in Lower Cretaceous sediments of the Neuquén Basin. Geological Society, London, Special Publications 252 (1), 231–250.
Scholle, P.A., BouDagher-Fadel, M., Ulmer-Scholle, D.S., Love, D.W., 2016. On the origin of carbonate nodules in the Bursum Formation at Cibola Spring, Socorro Country, New Mexico. In: New Mexico Geological Society Guidebook, 67th Field Conference, Geology of the Belen Area, pp. 369–376, 2016.
Schulte, S., Davaud, E., Wernli, R., 1993. Les bioconstructions à foraminiferes de l'Urgonien du massif Haut-Giffre (Hte Savoie, France). Bulletin de la Société géologique de France 164 (5), 675–682.

Scoffin, T.P., Stoddart, D.R., Tudhope, A.W., Woodroffe, C., 1985. Rhodoliths and coralliths of Muri Lagoon, Rarotonga, Cook Islands. Coral Reefs 4 (2), 71–80. https://doi.org/10.1007/BF00300865.

Shroba, C.S., 1993. Taphonomic features of benthic foraminifera in a temperate setting: experimental and field observations on the role of abrasion, solution and microboring in the destruction of foraminiferal tests. PALAIOS 8, 250–266. https://doi.org/10.2307/3515148.

Spalletti, L.A., Veiga, G.D., Schwarz, E., 2011. La Formación Agrio (Cretácico Temprano) en la Cuenca Neuquina. In: Relatorio del XVIII Congreso Geológico Argentino. Asociación Geológica Argentina, Buenos Aires, pp. 145–160.

Spalletti, L.A., Poiré, D.G., Schwarz, E., Veiga, G.D., 2001. Sedimentologic and sequence stratigraphic model of a Neocomian marine carbonate–siliciclastic ramp: Neuquén Basin, Argentina. Journal of South American Earth Sciences 14 (6), 609–624. https://doi.org/10.1016/S0895-9811(01)00039-6.

Schwarz, E., Veiga, G.D., Trentini, G.A., Spalletti, L.A., 2016. Climatically versus eustatically controlled, sediment-supply-driven cycles: carbonate–siliciclastic, high-frequency sequences in the Valanginian of the Neuquén Basin (Argentina). Journal of Sedimentary Research 86 (4), 312–335. https://doi.org/10.2110/jsr.2016.21.

Taylor, P.D., Wilson, M.A., 2003. Palaeoecology and evolution of marine hard substrate communities. Earth-Science Reviews 62 (1–2), 1–103. https://doi.org/10.1016/S0012-8252(02)00131-9.

Taylor, P.D., Lazo, D.G., Aguirre-Urreta, M.B., 2009. Lower Cretaceous bryozoans from Argentina: a 'by-catch'fauna from the Agrio Formation (Neuquén Basin). Cretaceous Research 30 (1), 193–203. https://doi.org/10.1016/j.cretres.2008.07.003.

Thalmann, H.E., 1951. Mitteilungen über Foraminiferen IX. Eclogae Geologicae Helvetiae 43 (1950), 221–225. https://www.e-periodica.ch/digbib/view?pid=egh-001:1950:43#275Tyson.

Tyson, R.V., Pearson, T.H., 1991. Modern and ancient continental shelf anoxia: an overview. Geological Society, Special Publication London 58 (1), 1–24. https://doi.org/10.1144/GSL.SP.1991.058.01.01.

Tyson, R.V., Esherwood, P., Pattison, K.A., 2005. Organic facies variations in the Valanginian-mid-Hauterivian interval of the Agrio Formation (Chos Malal area, Neuquén, Argentina): local significance and global context. Geological Society, London, Special Publications 252 (1), 251–266. https://doi.org/10.1144/GSL.SP.2005.252.01.12.

Toomey, D.F., Mitchell, R.W., Lowenstein, T.K., 1988. "Algal biscuits" from the Lower Permian Herington/Krider limestones of southern Kansas – northern Oklahoma; paleoecology and paleodepositional setting. PALAIOS 3 (3), 285–297. https://doi.org/10.2307/3514658.

Tucker, M.E., 1973. Ferromanganese nodules from the Devonian of the Montagne Noire (S. France) and West Germany. Geologische Rundschau 62 (1), 137–153. https://doi.org/10.1007/BF01826821.

Varrone, D., d'Atri, A., 2007. Acervulinid macroid and rhodolith facies in the Eocene nummulitic limestone of the Dauphinois Domain (Maritime Alps, Liguria, Italy). Swiss Journal of Geosciences 100 (3), 503–515. https://doi.org/10.1007/s00015-007-1239-8.

Veiga, G.D., Spalletti, L.A., Flint, S., 2002. Aeolian/fluvial interactions and high-resolution sequence stratigraphy of a non-marine lowstand wedge: the Avilé Member of the Agrio Formation (Lower Cretaceous), central Neuquén Basin, Argentina. Sedimentology 49, 1001–1019. https://doi.org/10.1046/j.1365-3091.2002.00487.x.

Vergani, G.D., Tankard, A.J., Belotti, H.J., Welsink, H.J., 1995. Tectonic evolution and paleogeography of the Neuquén Basin, Argentina. In: Tankard, A.J., Suárez, R., Welsink, H.J. (Eds.), Petroleum basins of South America., vol. 62. American Association of Petroleum Geologists, Memoir, pp. 383–402.

Weaver, C., 1931. Paleontology of the Jurassic and Cretaceous of West and Central Argentina, vol. 1. Memoir University of Washington, Seattle, p. 496.

Wei, H., Chen, D., Wang, J., Yu, H., Tucker, M.E., 2012. Organic accumulation in the lower Chihsia Formation (Middle Permian) of South China: constraints from pyrite morphology and multiple geochemical proxies. Palaeogeography, Palaeoclimatology, Palaeoecology 353, 73–86. https://doi.org/10.1016/j.palaeo.2012.07.005.

Wendt, J., 1969. Foraminiferen-'Riffe' im karnischen Hallstätter Kalk des Feuerkogels (Steiermark, Österreich). Paläontologische Zeitschrift 43, 177–193. https://doi.org/10.1007/BF02987650.

Wendt, J., 1974. Encrusting organisms in deep-sea manganese nodules. In: Hsü, K.J. (Ed.), Pelagic Sediments: on Land and under the Sea., vol. 1. International Association of Sedimentologists, pp. 437–447.

Wernli, R., Schulte, S., 1993. «*Bdelloidina*» *urgonensis* n. sp., un foraminifère constructeur de biohermes dans l'Urgonien de Haute-Savoie (France). Eclogae Geologicae Helvetiae 86 (2), 529–541.

Wignall, P.B., Newton, R., 1998. Pyrite framboid diameter as a measure of oxygen deficiency in ancient mudrocks. American Journal of Science 298 (7), 537–552.

Wignall, P.B., Newton, R., Brookfield, M.E., 2005. Pyrite framboid evidence for oxygen-poor deposition during the Permian–Triassic crisis in Kashmir. Palaeogeography, Palaeoclimatology, Palaeoecology 216 (3–4), 183–188. https://doi.org/10.1016/j.palaeo.2004.10.009.

Wilkin, R.T., Barnes, H.L., 1997. Formation processes of framboidal pyrite. Geochimica et Cosmochimica Acta 61 (2), 323–339. https://doi.org/10.1016/S0016-7037(96)00320-1.

Wilkin, R.T., Arthur, M.A., Dean, W.E., 1997. History of water-column anoxia in the Black Sea indicated by pyrite framboid size distributions. Earth and Planetary Science Letters 148 (3–4), 517–525. https://doi.org/10.1016/S0012-821X(97)00053-8.

Wilkin, R.T., Barnes, H.L., Brantley, S.L., 1996. The size distribution of framboidal pyrite in modern sediments: an indicator of redox conditions. Geochimica et Cosmochimica Acta 60 (20), 3897–3912.

Wilson, M.A., Palmer, T.J., 1992. Hardgrounds and hardground faunas, vol. 9. Institute of Earth Studies Publications, Aberystwyth, p. 131. University of Wales.